

The Use of NMR Based Metabolomics to Discriminate Patients with Viral Diseases



Banny Silva Barbosa Correia, Priscila Marques Firmiano Dalle Piagge, Luísa Souza Almeida, Gabriel Henrique Ribeiro, Cristina de Souza Peixoto, Luiz Alberto Colnago, and Daniel Rodrigues Cardoso

Abstract Infectious diseases are one of the most common conditions impacting global health, being a matter of concern for health agencies due to their contagious capacity and periodic outbreaks of new diseases, such as the global pandemic COVID-19. Viruses are among the main causes of this illness and it is defined as obligate intracellular parasites for their need to have a host cell to live and reproduce, since they won't produce proteins and compete for nutrients and metabolites leading to the alteration of the host metabolome. The diagnosis of these viral infections can be done by detecting viral particles or components, isolating the virus in cell culture, or even by evaluating immune responses. In this context, metabolomics comes as a very useful tool that reflects all “omics” techniques and best represents the phenotype. Since water-soluble metabolites and lipids are the major molecular constituents of human plasma, their abnormalities are commonly observed during disease, which contributes to the understanding of physiology and pathology. Nuclear magnetic resonance (NMR) spectroscopy and mass spectrometry (MS) are the most widely used techniques in metabolomics. NMR spectroscopy has emerged as a valuable application due to its ability to identify compounds with simple sample preparation, in addition, to being a non-destructive, highly reproducible, and quantitative technique (primary ratio method). These features make NMR a valuable tool that is frequently used in metabolomics analysis, and nowadays used in the diagnosis of viral diseases. Therefore, in this chapter, we will address a short integrative description of viral diseases and diagnostics, metabolomics, and NMR concepts. Furthermore, we will explore the advances in NMR-based metabolomics applied in medicine, and finally, the viral diseases discriminated by NMR-based metabolomics.

Keywords NMR · Metabolomics · Viral diseases · Prognosis

B. S. B. Correia · P. M. F. D. Piagge · L. S. Almeida · C. de Souza Peixoto · D. R. Cardoso (✉)
University of Sao Paulo, Chemistry Institute of Sao Carlos, São Carlos, Sao Paulo 13560-970, CP
780, Brazil
e-mail: drcardoso@iqsc.usp.br

G. H. Ribeiro · L. A. Colnago
Embrapa Instrumentation, Brazilian Agricultural Research Corporation, Sao Carlos, Sao
Paulo 13570-970, Brazil

1 Introduction

Viruses are one of the major causes of human diseases, ranging from mild to several symptoms including death. Influenza viruses have been the most lethal viruses since early 1900. More recently, Acquired Immune Deficiency Syndrome (AIDS) caused by the human immunodeficiency virus (HIV), and COVID-19, caused by the human coronavirus SARS-CoV2 have been the major new virus diseases affecting people around the world. COVID-19 has been declared a pandemic by the World Health Organization (WHO) in March 2020 and until March 2022 (2 years later) caused 6 million people to die [1]. Other viral outbreaks causing severe symptoms and death have emerged in recent decades including Dengue, Zika, and Ebola viruses. Table 1 shows the most common human viral diseases worldwide, their clinical manifestations, and their detection methods [2–21].

Viruses are structures formed by proteins and other compounds that encapsulate DNA or RNA molecules. Therefore, viruses don't have the biological machinery to self-replicate and consequently, they have to infect a specific living cell to use their replicating machinery to form new virus particles and continue the infection process [22]. Consequently, the metabolism of infected cells is strongly affected by virus replication. In multicellular organisms, like animals and plants, virus infections may strongly affect the metabolism of the entire being. Therefore, the metabolomics approach can be a useful technique to monitor the virus's infection and the organism's response to the infection.

1.1 Metabolomics

Cells are constantly involved in a great variety of chemical reactions, acting on intra- and extracellular communication to provide essential biochemical processes for the survival of the organism as a whole, such as protection and energy. Every single reaction is linked in its way to one another, resulting in a complex network, formed by lots of different pathways. Therefore, metabolism is defined as a set of interconnected biochemical reactions that requires a collective and complementary work of all pathways [23].

Each molecule in the complex network of metabolism has its function, such as signalize other molecules to start a reaction/process. Most biochemical reactions in a metabolic system don't present a pattern and spontaneous behavior since it is considered an open system, which is in constant energy exchange. Hence, released energy from a reaction contributes to the facilitation of another reaction. Enzymes can also act as a facilitator, since they withhold the capacity of catalyzing a reaction, lowering the activation energy barrier required for a given reaction, allowing it to proceed without changing the original arrangement of the facilitator [23].

Metabolic pathways may always provide a synthesis or decomposition of some components of the organism. Anabolism is a set of pathways that requires a load of

Table 1 Most common human viral diseases, their clinical manifestations, and their detection methods [2–21]

Disease	Viral pathogenic	Symptoms	Detection method
Acquired immune deficiency syndrome (AIDS)	Human immunodeficiency virus (HIV)	Fever, malaise, sore throat, muscle pain, and rash	ELISA
Chickenpox	Varicella-zoster virus (VZV)	Fever, headache, fatigue, pharyngitis, and blisters on the chest, back, and face	PCR
Common cold	Rhinovirus (HRV)	Nasal congestion, runny nose, sneezing, headache, cough, and sore throat	Observation of the symptoms' progression
COVID-19	Coronavirus (SARS-CoV-2)	Fever, fatigue, cough, weakness, nausea, vomiting, diarrhea, shortness of breath, and changes to taste and smell	RT-PCR
Dengue	Dengue virus (DENV)	Severe headache, swollen glands, nausea, vomiting, rash, muscle, joint, and behind the eyes pain	PCR and ELISA
Ebola virus disease (EVD)	Ebolavirus (EBV)	Fever, fatigue, headache, sore throat, vomiting, diarrhea, rash, and muscle pain	RT-PCR and ELISA
Genital warts	Human papillomavirus (HPV)	Sore throat, earache, neck mass, and warts in the genital area	Biopsy
Hepatitis B	Hepatitis B virus (HBV)	Fatigue, nausea, vomiting, abdominal pain, dark urine, and jaundice	ELISA
Hepatitis C	Hepatitis C virus (HCV)	Fatigue, weakness, nausea weight loss, anorexia, joint, and muscle pain	PCR and ELISA
Infectious Mononucleosis	Epstein-Barr virus (EBV)	Fever, headache, splenomegaly, lymphadenopathy, and sore throat	Immunofluorescent test
Influenza A	Influenza A virus (IAV)	Fever, malaise, cough, sore throat, runny nose, muscle, and joint pain	RT-PCR and viral culture

(continued)

Table 1 (continued)

Disease	Viral pathogenic	Symptoms	Detection method
Measles	Measles virus (MV)	Fever, headache, abdominal and pharynx pain, photophobia, swelling of lymph nodes, coryza, cough, and conjunctivitis	ELISA and viral culture
Mumps	Mumps virus (MuV)	Fever, headache, malaise, anorexia, parotid swelling, and muscle pain	RT-PCR and immunofluorescent test
Oral Herpes	Herpes simplex virus (HSV)	Fever, muscle pain, headache, swollen lymph nodes, and blisters or ulcers at the oral mucosa	Viral culture
Poliomyelitis	Poliovirus (PV)	Fever, fatigue, headache, vomiting, limb pain, and stiff neck, followed by paralysis	PCR and viral culture
Rabies	Rabies virus (RABV)	Fever, pain, and paraesthesia around the wound site	RT-PCR
Respiratory viral sepsis	Adenovirus (ADV)	Fever, cough, sore throat, nasal congestion, and runny nose	PCR and viral culture
Smallpox	Variola virus	Fever, headache, backache, abdominal pain, vomiting, rashes on the face, arms's and legs	PCR and viral culture
Yellow fever	Yellow fever virus (YFV)	Fever, fatigue, headache, nausea, vomiting, jaundice, and muscle pain	PCR and ELISA
Zika fever	Zika virus (ZIKV)	Fever, headache, sore throat, conjunctivitis, rash, joint, and muscle pain	PCR

PCR: polymerase chain reaction, **RT-PCR:** reverse transcription-polymerase chain reaction, **ELISA:** enzyme-linked immunosorbent assay

energy to complete the synthesis of complex molecules, using smaller and simpler ones as precursors. On the other hand, catabolism presents a collection of pathways that performs the rupture of chemical bonds, creating some small molecules from one complex structure to create energy-storing molecules, which can be used in anabolic pathways in an endless cycle [23].

Metabolites are the byproduct or the intermediate of such metabolic process. As the final product of a reaction, these compounds may indicate disturbances in some specific pathways, since it reflects each alteration that the organism has suffered because the organism will contribute in a different way to the formation or decomposition of these small molecules. Thus, metabolites analysis may offer a complete vision of one's phenotypical responses that other macromolecules cannot. Proteins may suffer post-transcriptional adaptations, as well as genes, may suffer epigenetic regulations, making it difficult to directly correlate these macromolecules with the organism's phenotypic behavior [23].

Metabolomics is an emerging field within the "omics" sciences, concerning the biochemical processes that take place within a cell, tissue, or organism, involving a specific group of metabolites in a metabolome, as an approach to assimilating biological mechanisms and map functions of metabolic pathways. Metabolites profile and/or levels being monitored can help predict the biological structure, as well as the function, of a phenotype, leading to the understanding of the response of the organism to environmental stressors, such as nourishment, exposure to toxins and infections, that lead to perturbations in cellular homeostasis. Since the phenotype is directly linked to the genotype and its behavior, genetic variations will also generate phenotypic variations [24–26].

To develop an experimental study using this "omics" technique, some basic steps must be performed as illustrate in Fig. 1. Before starting the metabolomics analysis, the determination of the study strategies and the design of the experiments are required. Untargeted metabolomics is a methodology based on the global profiling of all the metabolites in a biological sample, including chemical unknowns, whereas targeted methodology presents a more specific approach, with a characterized metabolite as a valid standard, focusing on particular metabolites signals. The study strategies can be developed from one of these concepts in an arrangement with the most appropriate analytical techniques [25, 26].

Furthermore, a large amount of biochemical information gathered can be correlated through statistical and chemometric analysis. Metabolomics samples carry a complex load of metabolites, which generates cross information that can't be visualized considering individual biomarkers. Data analysis greatly depends on preprocessing, which has the aim of transforming the data to improve the data analysis through a simplification of the dataset to be comparable [25].

After data preprocessing, several statistical tools can be used to find discriminative features within the sample set. Data analysis involves the application of the different univariate and multivariate methods that can be of parametric (e.g. student *t*-test, multivariate linear regression) or non-parametric (e.g. Mann–Whitney test, random forests) nature. The methods can be also divided into unsupervised techniques (i.e. methods where labeling of the samples is not involved in calculations, e.g. principal

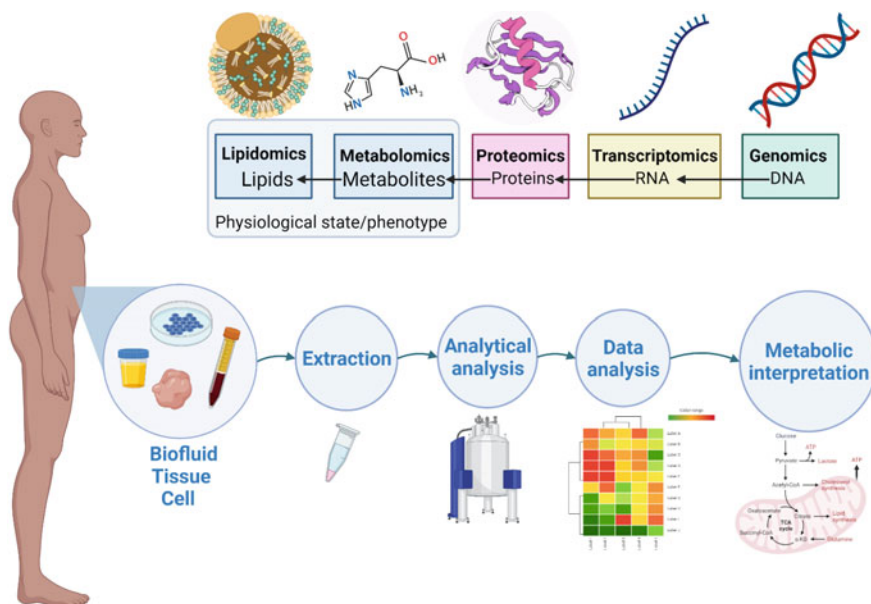


Fig. 1 Metabolomics scheme showing the sequence of macromolecules to small molecules and their respective omics science, the metabolomics steps from the human sample as biofluid, tissue or cell until final results as metabolic interpretation. Created with Biorender.com

component analysis (PCA), hierarchical cluster analysis (HCA), and supervised techniques (i.e. methods where calculations involve the information regarding sample labels, e.g. linear discriminant analysis (LDA), k-nearest neighbor (KNN). A supervised multivariate technique, partial least squares discriminant analysis (PLS-DA), is a particularly useful tool in metabolomics studies [27].

The application of statistical analysis aims to see a general correlation between the metabolites in a simpler interpretation. Principal Components Analysis (PCA) is commonly used in these cases for its ability to reduce the range of a database, minimizing information loss while retaining the main features. In a PCA plot, it is possible to analyze similarities and differences between samples and the control, considering the distance between the points. On the other hand, ANOVA and Student's *t*-test, with a *P*-value of < 0.05 , are univariate analyses that can be used to analyze the parameters of an isolated metabolite, since it doesn't depend on other variables [25].

Scores and loadings are the usual visual results from the multi statistical analyses in which the scores describe samples and the loadings show the features. The scores must present a cluster (group) or a tendency for a cluster to claim that the metabolites are distinct in the different samples. Loadings features correlating with score clusters are relevant to establishing what metabolites distinguish the samples. Thus, the feature may be presented as clearly as possible with the aim of emphasising which metabolites are important. One of the possible loading charts is the heatmaps based on VIP (variable importance in projection) [28].

For metabolism investigation, the Pathway Analysis is used which module combines results from powerful pathway enrichment analysis with pathway topology analysis to help researchers identify the most relevant pathways involved in the conditions under study. This analysis uses enrichment techniques as key tools for understanding complex biological systems. These tools reduce the complexity of the data, improve interpretation and understanding of biological systems, and help to generate hypotheses. The presentation of the pathways usually is a map of the metabolome view [29].

1.2 NMR as a Tool in Metabolomics

There are several analytical tools to study metabolomics, among them, the most used are nuclear magnetic resonance (NMR) and mass spectrometry (MS). MS has excellent sensitivity, and a large coverage of metabolites, and can be coupled with separation techniques, being important for the analysis and identification of a wide variety of compounds, but reproducibility and quantitation is a current issue. However, in this chapter we will delve deeper into the use of NMR in metabolomic analysis, addressing the operation and the main advantages of the technique [30–32].

Nuclear magnetic resonance (NMR) spectroscopy is a rapid and non-destructive technique that allows a high analytical reproducibility, identification of chemical compounds without the use of standards, and information about molecular dynamics. NMR can detect a gamma of metabolites in a complex sample with minimal sample preparation when compared to other analytical methods [33, 34].

When it comes to the actual experiment in human beings, the samples can be collected as biofluids (urine, saliva, blood, plasma, serum, cerebrospinal fluid, stool) or also as tissues (biopsy tissue), and cells. To obtain a sample with minimal alterations for reproducible experiments, the preparation is quite simple. It starts with the homogenization of the collected sample by the centrifuge followed by the metabolite's extraction, adding some deuterated solvent. The extraction of metabolites can also be promoted by the biomolecules' precipitation, as a result of the addition of methanol: chloroform mixture, or only the methanol itself, that also provides the inactivation of enzymes. After that, the sample is centrifuged and the floating part is evaporated. Then, the reference standard is added, as well as the deuterated solvent or buffer is added. It is important to maintain the physiological pH during the sample preparation, since its variation may induce unwanted reactions [35].

In the final step samples can be filtered or not to remove macromolecules that may get in the way during the spectral analysis. If the macromolecules are not physically removed, the choice of NMR experiment must be well planned (a Carr-Purcell-Meiboom-Gill—CPMG—pulse sequence must be required). The samples are transferred to the equipment's tubes and the analysis may begin. It is important to avoid a sequence of thawing processes under the same sample. At the end of this process, it is obtained a well-preserved biological sample, making it possible to

use nuclear magnetic resonance (NMR) as the analytical technique, since it is non-destructive and allows other types of analysis later, or the reproduction of the same one. Less processed samples provide a result loaded with information, with larger width and more overlaps, as well as the possibility to correlate all these features in a bigger view analysis. Besides, a rawer sample supports the idea of a replicable experiment, since it hasn't been overly modified, and is best used in NMR analysis [36]. A graphical illustration of the sample handling process is available in Fig. 2.

Several nuclei can be studied by the NMR, but the most commonly available ones are hydrogen-1 and carbon-13 isotopes [37, 38]. One-dimension ^1H and ^{13}C are the most common NMR experiments. More sophisticated multidimensional experiments involving for example ^1H - ^1H and ^1H - ^{13}C , such as COSY (correlated spectroscopy) and HSQC (heteronuclear single quantum coherence) [38] among many others also are common. Solution or liquid-state NMR, and HR-MAS (High-Resolution Magic Angle Spinning) are the two main approaches employed in metabolomics. Solution NMR is used in the analyses of soluble metabolites in biofluids, cell lysates, or polar/apolar tissue extracts, and HR-MAS for the measurement of metabolites in heterogeneous samples containing solid and liquid components, like intact tissues [39].

Liquid-state NMR in high resolution (600 MHz) is the preferred instrument to perform metabolomics analyses in biological samples containing many compounds

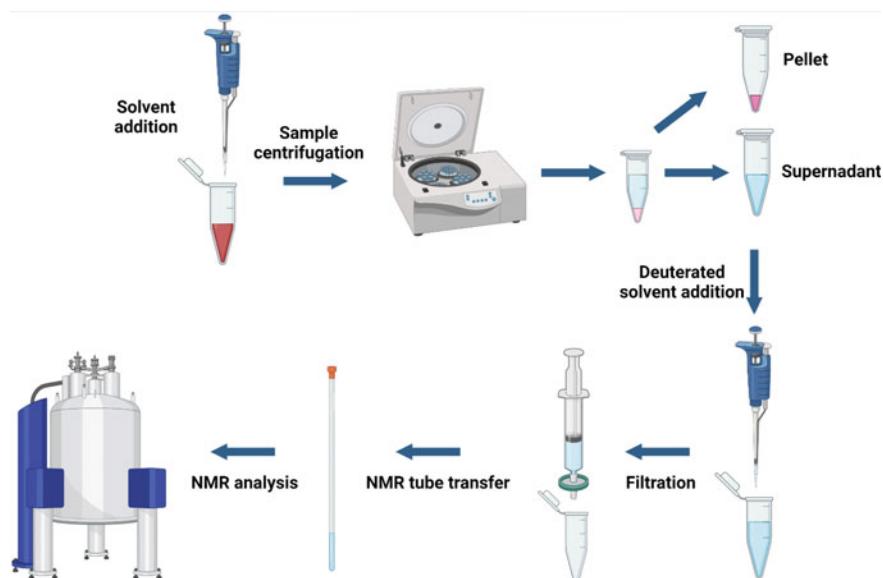


Fig. 2 Representation of sample handling process to NMR-based metabolomics analysis. Initially, the solvent is added for protein precipitation, centrifugation, and separation of the supernatant and pellet fractions. Then, a deuterated solvent is added to the supernatant, followed by filtration, insertion of the sample into the NMR tube and, finally, the sample is inserted and analyzed in the NMR spectrometer. Created with Biorender.com

in different degrees of abundance. Usually, ^1H NMR the spectrum is acquired with a pulse sequence including water presaturation to suppress the solvent signal [39–42]. Additionally, in selected samples, some bidimensional experiments, usually COSY, HSQC, and JRES are performed to aid the process of metabolites identification. The metabolites identification relies on the comparison of chemical shifts, and spin–spin couplings to information available in chemical databases such as HMDB, Chenomx NMR Suite (Chenomx, Canada), and literature [27]. After carrying out all the steps described, it is possible to obtain a spectrum as shown in Fig. 3.

Under appropriate quantitative NMR (qNMR) conditions, NMR spectra may provide direct quantitative information since the area of each signal in the spectrum is directly proportional to the number of equivalent nuclei responsible for that signal, or in other words, is directly proportional to the molar amount of the detected isotope nuclei [37, 43]. Thus, absolute concentrations of the metabolites can be determined by NMR using internal, external, or electronic generated signal [33, 43, 44].

The qNMR spectra must be acquired under a set of appropriate conditions to obtain accurate results. For a maximum error of 1% it is necessary to set the relaxation delay (delay before the excitation) equal to at least 5 times the longitudinal relaxation time (T_1) for a 90° pulse, and an acquisition time longer than 3 times the transverse relaxation time (T_2), and at least 50:1 signal to noise ratio. Careful processing of NMR spectra is also required to extract accurate peak areas [33, 37].

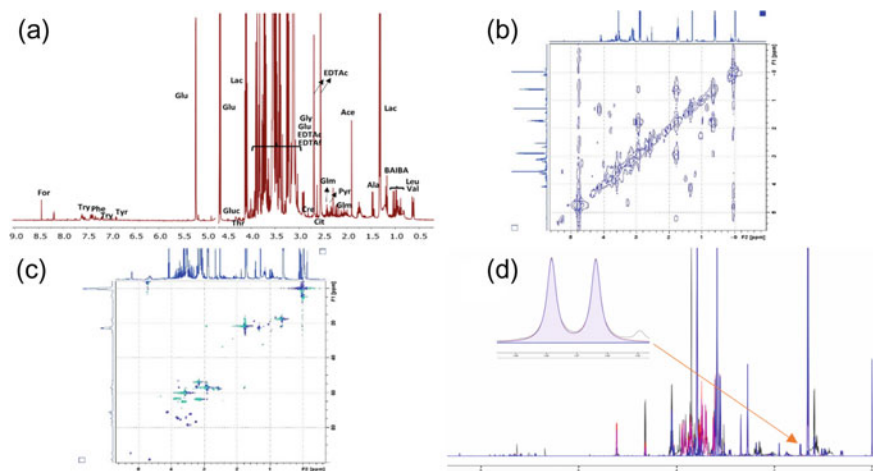


Fig. 3 Spectra ^1H NMR and bidimensional experiments were obtained from blood plasma samples of covid-19 patients at the time of hospitalization. **a** ^1H NMR spectrum with identification of the most intense metabolites; **b** Correlation Spectroscopy (COSY) showing scalar couplings between hydrogen atoms; **c** Heteronuclear Single Quantum Correlation (HSQC) showing the correlations between carbon and hydrogen nuclei that are directly bonded; **d** Quantification by Chenomx NMR Suite (professional version 8.1). Superposition of the obtained spectrum (black line) with the software library containing the reference compounds (filled in blue) allows spectral deconvolution, identification, and individual quantification of metabolites

NMR spectra preprocessing usually involves baseline correction, alignment, binning, normalization, and scaling [28].

2 Advances in NMR Based Metabolomics to Apply to Diagnostic Diseases

As mentioned so far, metabolomics is an efficient tool to optimize viral disease metabolome profiling overdue the generation of detailed chemical pathology fingerprints enabling the association to diagnostic and therapeutic interventions [45]. This personalized approach in medicine is probably the most important paradigm change in medical diagnosis and appears to be the future of modern medicine [46]. Hence, to improve its performance and promote a gradual transition from standardized clinical protocols to personalized medicine. NMR Metabolomics has been improving its methodologies to obtain better data resolution, avoid peak overlap, improve sensitivity, and also maintain an auto sustainable work regarding the high demands in clinical studies as a semi- or fully-automatization process from preparation steps to data results.

Regarding the NMR acquisition to improve data quality, researchers in the past decade studied and validated advanced NMR experiments through different approaches (1D and multidimensional NMR). Considering that biofluids are a complex matrix that not only comprises small metabolites but is also rich in proteins and lipids, applying a diffusion-edited pulse sequence like Carr-Purcell-Meiboom-Gill (CPMG) for the NMR analysis is typically necessary, suppressing the protein and lipids signals and allowing the analysis of small molecules without matrix interference. The CPMG does not represent the last advance, however worth mentioning once certainly was the historical advance in biofluids analysis.

The CPMG relies on molecules' transversal relaxation time (T_2). A spin-oriented chemical compound under an external magnetic field presents a longitudinal (T_1) and a transversal (T_2) relaxation rate - back to the z and y-axis, respectively. These properties are related to the magnetization axis the spin is oriented. CPMG pulse sequence starts with a 90° pulse to the y axis. The time required for the spin to lose its magnetization on the transversal axis (y) is smaller in macromolecules, compared to small molecules. Hence, to record only small molecules of T_2 , there is a sequence of 180° pulses and a T time acting as a spin echo. This enables the NMR equipment to filter T_2 on samples [47, 48].

However, this CPMG approach commonly causes a broadening of the baseline, complicating posterior quantitative data analysis [35]. Alternatives to avoid this problem is physically removing the macromolecules from the samples [36, 45] or balancing the fast data and efficiency within additional experiments, which is the case with the use of the Bruker proprietary In Vitro Diagnostics research (IVDr) method for the entire biofluid sample [35].

Considering saving time while handling hundreds of samples, research using the newest NMR Bruker metabolomics protocol named In Vitro Diagnostic research (IVDr) to characterize the metabolic profile and quantify metabolites in biofluids samples seems to be the latest innovation in viral diseases metabolomics.

As shown in Fig. 4, for IVDr protocol the instrument is calibrated before the analysis, and the automated methods are performed on each sample. For plasma sample, IVDr performs four experiments in automation mode: a standard 1D experiment with solvent presaturation (noesy); a 1D—Carr – Purcell – Meiboom – Gill (CPMG) spin – echo experiment; a 2D—J-resolved experiment, and a 1D diffusion-edited spectrum. The methods rely on using short relaxation times within some corrector factor strategy to expedite quantitative analysis. The quantification data is automatically calculated for a standard metabolite list for each biofluid (blood, urine, and cerebral spinal fluid—CSF) based on the electronic signal ERETIC (Electronic Reference To access In vivo Concentrations) [49].

Novel IVDr protocols focus on fast and efficient quantification profiles of both small metabolites and lipoprotein fractions [50]. Elaine Holmes, John Lindon, and Jeremy Nicholson group have reported a series of studies trying to provide a standard protocol for IVDr methodology to ensure its reproducibility and robustness [45, 50–52]. This strategy showed to be appropriate for the SARS-CoV-2 metabolic profile due to previous reports of the high demand for lipid metabolism on Covid-19 pathology. Their results are promising for the differentiation of SARS-CoV-2 infected patients from healthy patients based on lipid profile (Table 2). They could also relate cytokine levels in both groups and compare them with lipid quantification and the disease evolution [53]. More about Covid-19 studies are discussed in Sect. 3.1.

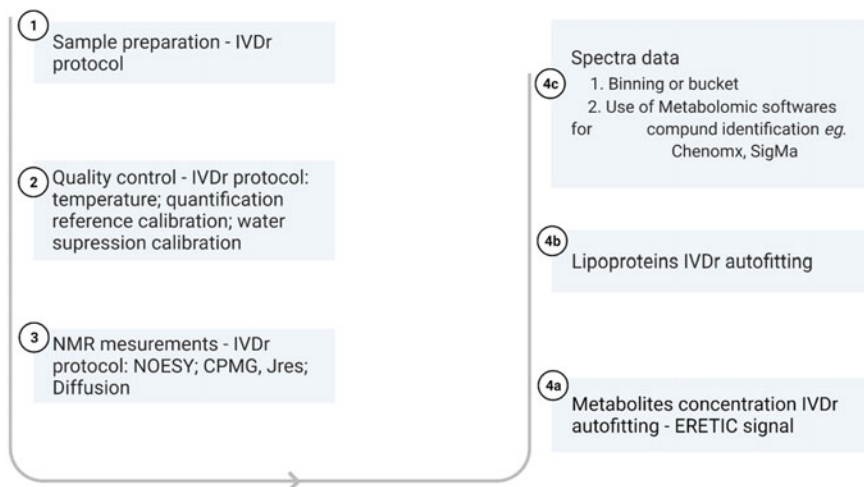


Fig. 4 Scheme showing the Bruker IVDr protocol analysis steps to perform metabolomics analysis

Table 2 Distinct metabolite types for SARS-CoV-2 infected patients from healthy patients

Group	Metabolites in abundance
SARS-CoV-2 infected patients	LDL cholesterol (LDCH), LDL phospholipids (LDPL), LDL-free cholesterol (LDFC), LDL apolipoprotein B, HDL cholesterol (HDCH), and phospholipids (HDPL)
Healthy patients	VLDL cholesterol (V1CH, V2CH, and so forth) and triglycerides (V1TG, V2TG, and so forth)

Metabolites assigned by PCA analysis. Data extract from Lodge's paper [53]

Besides the advantage of fast data acquisition to cohort studies samples, IVDr enables NMR metabolomics researchers to manage multivariate data from different centers and compare their data due to the IVDr protocol required to be the same, making it a universal protocol. One example is the cooperation between the Australian National Phenome Center (ANPC) with Bruker in an attempt to deliver COVID-19 diagnostic and prognostic solutions [54].

Many efforts have been putting on mainly in metabolomics data, more precisely in metabolites identification. Standardized methods were created such as SigMa which focuses on analyzing biofluids Lipoproteins, LipSpin which are lipidic NMR databases, Chenomx, and COLMARm whose software identifies and quantifies small metabolites [55, 56].

2.1 *qNMR Strategies to Overcome the Metabolomics Issues*

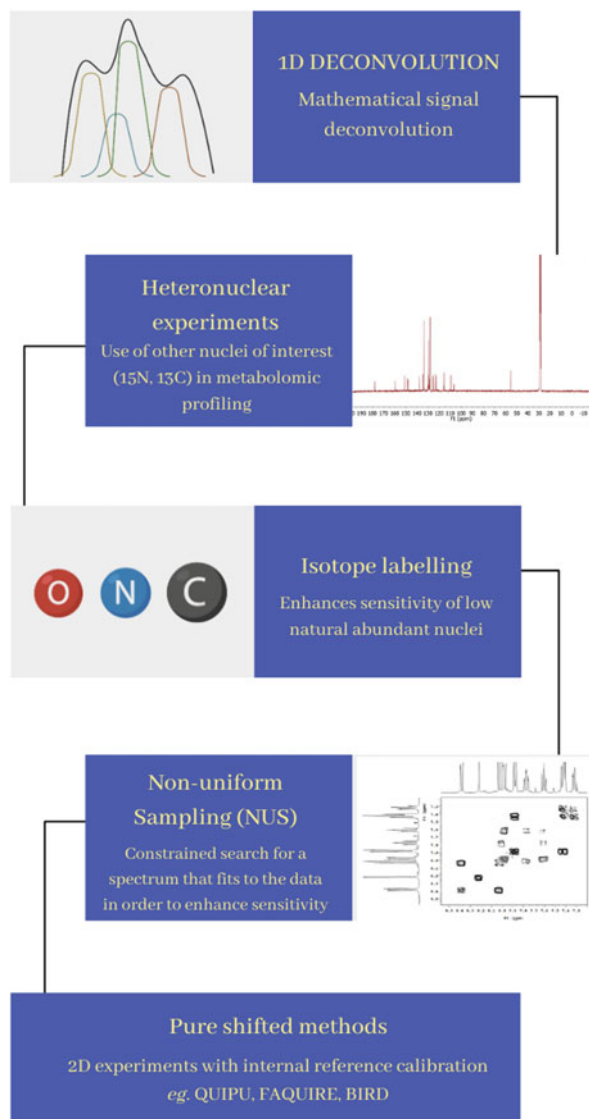
The accurate quantitation of larger numbers of metabolites has some challenges. The overlapping signals and lower sensitivity continue to be a struggle in metabolomics. To overcome these issues some strategies are being developed and explored by researchers (Fig. 5) [44, 57].

Strategy 1 consists of the 1D NMR solutions to spectrum overlapped issues involving deconvolution and heteronuclear experiments [58]. Deconvolution experiments use mathematical deconvolution of 1D NMR line shapes to separate individual 1D spectra of the different analytes present in the sample; while heteronuclear experiments separate the data at the acquisition stage using another nucleus, such as ^{13}C , ^{15}N , ^{31}P , or ^{17}O , different of ^1H [38, 44]. In the meantime, 1D NMR with isotope labeling is another strategy to not only identify a metabolite set but also track down their metabolic pathway and cell influx/efflux. This is a methodology that alleviates a major challenge in NMR experiments involving low natural abundant nuclei, which could involve the isotopes of ^{13}C , ^{15}N , ^2H [59]. The use of labeling ^{13}C quantitative one-dimensional HMQC (Q-1D-HMQC) ^1H NMR analysis has been reported for HBV infection. The combination of an isotope labeling and quantification technique provided a quantitative pathway description of this disease and made it possible to point out discussions about HBV infection [60]. Yet, isotope labeling improves

Fig. 5 Scheme illustrating the qNMR strategies to overcome the metabolomics limitations in the quantitative approach

qNMR STRATEGIES

Different 1D and 2D NMR experiments to overcome signal overlapping and enhance sensitivity



the technique sensitivity, overcoming a major problem in heteronuclear experiments [61].

The deconvolution of peak areas is an efficient alternative to simple data integration when peaks are overlapped, as described in Fig. 6 [27, 37]. The deconvolution method achieves the integration of the signals more accurately in 1D spectra since errors are minimized in quantitative parameters such as noise in the NMR spectrum, phasing errors, baseline approximation, and also, careless adjustment of slope and bias correction on integrals [37, 43]. In deconvolution, a peak (or peaks) is fitted to the observed spectrum using, for instance, a least-squares-based method. Initial values for line-fitting analysis (frequency, width, height, and line shape of a signal) can be either defined manually or obtained from a database that contains the model spectra of the compounds. The spectral parameters can be fitted depending on the software as shown in many scientific articles [37, 62].

Strategie 2 and 3 consist in expanding the 1D spectrum to another dimension, running a two-dimensional (2D) experiment regarding the factors that influenced the peak areas as the peaks are spread along with one (or more) orthogonal dimension(s) [37, 38, 44]. 2D NMR solutions are also available for qNMR, which can involve pulse sequence modifications, theoretical calculations, or calibration approaches with fast 2D acquisition methods, all carefully thought to account for the peak-specific response of the 2D NMR signal. The quantitative application of 2D NMR in the field of metabolomics is recent, and already are being developed more practical approaches. The intrinsically quantitative 2D NMR method is one of them [38].

The intrinsically quantitative 2D NMR method development relies on the use of a simple internal reference without the need to rely on multiple external standards, which would directly yield quantitative results in a way similar to 1D NMR. The “intrinsically” quantitative 2D approaches such as qHSQC and its variants and applications of pure shifted and NUS (nonuniform sampling) methods to 2D NMR experiments are strongly investigated [43, 63, 64].

Despite the benefits of the methods mentioned above, conventional 2D NMR suffers from long acquisition times because of the need to repeat numerous 1D

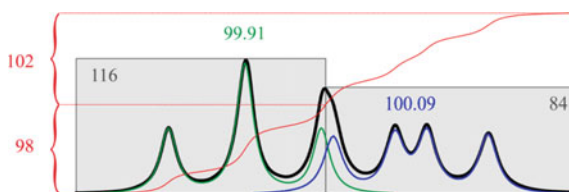


Fig. 6 Different methods to determine peak areas. The black line represents the observed spectrum where a triplet (t) and a doublet of doublets (dd) are overlapping. The red curve is the step curve used in the classical integration, in which their relative step heights determine the areas of 98 and 102 for the t and dd, respectively. Using the two bins from the equidistant binning procedure (grey boxes) areas of 116, and 84 for the t and dd were found, respectively. The most accurate results were obtained with deconvolution: the area of the t (green line) is 99.91 and the area of the dd (blue line) is 100.09. Reprinted with permission from Soinen et al. [37]

experiments with incremented delays to obtain a well-resolved 2D matrix. Therefore, many NMR methods have been developed to reduce the acquisition time of multi-dimensional experiments [44, 65]. Two main strategies seem to be a solution to overcome this situation: reducing the interscan sequence delay, e.g. band-Selective Optimized-Flip-Angle Short-Transient (SOFAST), Acceleration by Sharing Adjacent Polarization (ASAP), and Small Recovery Times (SMART). Another option is to introduce multiplexing instead of sequential sampling in the indirect dimension, by spatial encoding [61], as occurs in the ultrafast (UF) 2D NMR.

An operator must weigh the benefits of those first alternatives to attend to their research demand. SOFAST sequence is applied in HMQC experiments with an excitation pulse within a flip angle leading to a partial restoration of proton magnetization by a subsequent 180° pulse. This leads to an increased signal-to-noise ratio for high repetition rates of the experiment, nevertheless, SOFAST only is efficient for systems in which spin diffusion is an effective relaxation mechanism, such as macromolecules or small molecules in viscous solvents [61, 66]. ASAP sequence for HMQC relies on proton-proton coupling while a mixing stage retains the residual Z-magnetization. It is an advantage for small molecules, nonetheless, this sequence is restricted to heteronuclear experiments for samples at natural abundance or slightly enriched [61, 67]. SMART sequence eliminates artifacts from previous scans in 2D experiments through a pulse field gradient (on the x, y, and z-axis), dephasing them (Fig. 7). It could be applied for COSY and TOCSY sequences. Despite the use of smaller recovery delay times, it requires rather high concentrations and access to triple axis gradients [61, 68]. Within the approaches mentioned, medical studies were reported studying macromolecules and hormones. The evaluations performed so far were focused on chronic metabolites syndromes [69, 70]. These studies may enable further metabolic investigation in biofluids.

The ultrafast (UF) 2D NMR is a generic approach that can record any kind of 2D experiment in a fraction of a second as shown in Fig. 8 [38, 71].

The ultrafast (UF) 2D NMR proposes to reduce the sampling of the indirect time domain by recording the complete 2D NMR dataset in a single scan. This can relatively decrease the sensitivity, however, this can be solved by relying on hybrid methods offering a reasonable compromise between the experiment duration

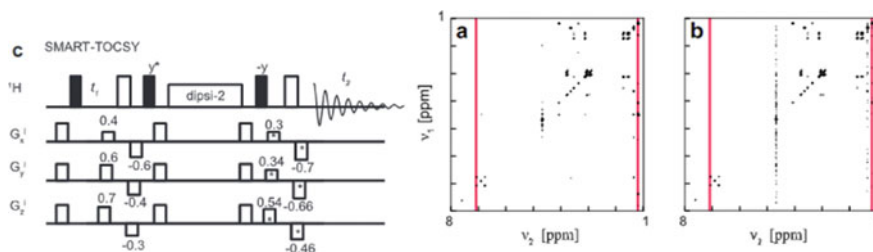


Fig. 7 SMART pulse sequence for a TOCSY **a** experiment. Comparison of a regular TOCSY **b** spectra and a SMART TOCSY **c** spectra containing Alanine, Arginine, Histidine, Threonine, and Tyrosine. Reprinted (adapted) with permission from [68]

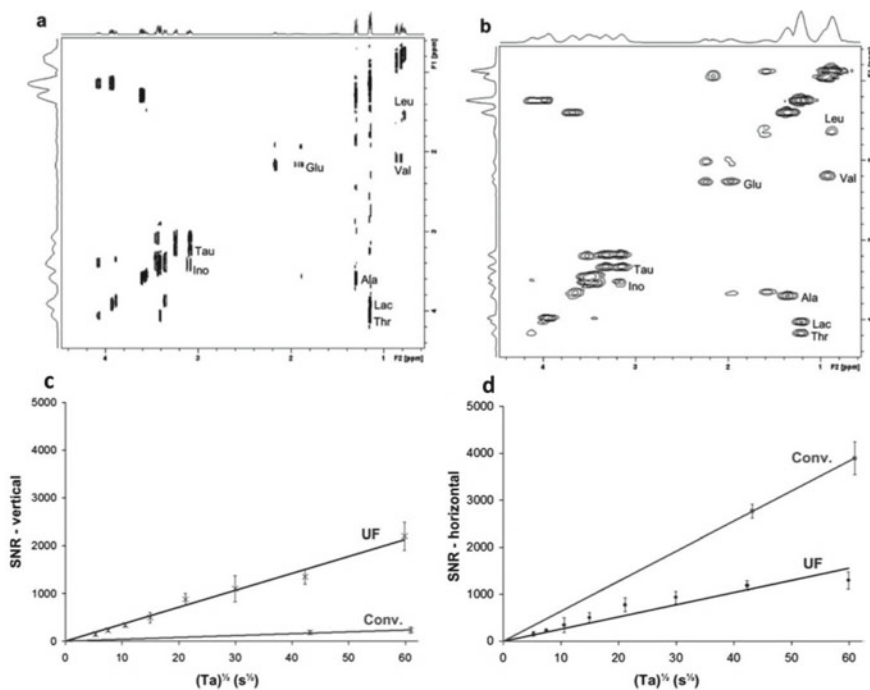


Fig. 8 Conventional **a** and ultrafast **b** COSY spectra of a 5 mM metabolic mixture of Alanine, Glutamic acid, Inositol, Lactic acid, Leucine, Taurine, Threonine, and Valine, acquire in 34 min on a 500 MHz spectrometer with a cryoprobe. Signal-to-noise ratio (SNR) as a function of the acquisition time, in the vertical **c** and horizontal **d** dimension of ultrafast (UF) and conventional (Conv.) constant-time COSY. Reprinted (adapted) with permission from [71]. Copyright 2011 Royal Chemical Society

(a few minutes) and the sensitivity (micromolar concentrations can be detected on homonuclear 2D spectra of biological extracts) [71]. The ultrafast method must be allied to the external calibration approach. Despite the similarity with other analytical methods, here the calibration curve is obtained from a single series of standard samples containing all the targeted analytes in known concentrations for each peak of interest [44]. Thus, hundreds of samples can be analyzed from the same calibration curves if the experiment is repeatable, leading to a fast method as reported in many scientific articles [44, 72–74].

Guenec and coworkers have presented the application of these experiments to cancer cells. The UF NMR could assign metabolites, most of the amino acids, in three different cell lines. Their results could be exploited in biological fluids due to the efficiency of UF NMR to identify metabolites in complex mixtures and point out their concentration [75].

There are quantitative 2D methods using a simple internal reference and without the need to rely on multiple external standards which would directly yield quantitative results in a way similar to 1D NMR. The “intrinsically” quantitative 2D approaches

such as Q HSQC and its variants (HSQC₀, or Q QUIPU HSQC) were developed to yield quantitative data from a single 2D spectrum [63, 64]. These approaches all rely on the HSQC pulse sequence. Therefore, they offer a better separation than UF COSY, thanks to the broader ¹³C chemical shift range, but they are also less sensitive due to the low natural abundance of ¹³C.

The QUIPU HSQC (QUantitative Perfected and pUre shifted HSQC) method is strongly recommended when strong overlap occurs once 2D ¹H, ¹³C NMR allows an enhancement of the spectral resolution compared to ¹H homonuclear 2D NMR (2D COSY), and an enhancement of the sensitivity compared to Q HSQC. However, this method consumes time due to the 2D acquisition mode combined with the long recycling times required by the quantitative requirements (5 times the longest longitudinal relaxation time T₁), and due to the higher number of scans needed to access low concentrated metabolites [63]. Additionally, the Bilinear Rotational Decoupling (BIRD) HSQC method stands as a prominent strategy to enhance spectral resolution and avoid sensitivity loss. This experiment uses a pulse sequence with a double spin-echo containing a bilinear rotational decoupling pulse cluster and a non-selective 180° proton pulse. This strategy provides a J-selective spin inversion and enhances the signal-to-noise ratio with isotope labeling and proved to be an effective tool for multidimensional NMR metabolomics analysis [76, 77].

The Nantes group has developed an accelerated version of this experiment named FAQUIRE (FAst, QUantitative, hIghly Resolved and sEnsitivity enhanced NMR) [63], an approach that combines the Q QUIPU (quick QUIPU) with spectral aliasing, NUS (nonuniform sampling), and VRT (variable repetition time) methods. The FAQUIRE approach promises to accelerate the access to quantitative data based on ¹H, ¹³C correlations while preserving the spectral resolution and the sensitivity, without the need for external calibration.

In Fig. 9 we show that the acquisition time of 2D quantitative maps using the FAQUIRE approach is reduced by a factor of 6–9 while conserving a high spectral resolution due to the pure shift approach. The “pure shift” spectrum is generated when homonuclear broadband decoupling is applied resulting in a greatly simplified NMR spectrum with the multiplet pattern removed [43]. Even so, this approach may result in sensitivity loss due to the selective J-refocusing elements [76]. The pure shift concept can be applied in both dimensions in a 2D NMR experiment.

3 Viral Diseases Discriminated by NMR Based Metabolomics

In this section, the scientific findings in the use of NMR-based metabolomics approaches for viral diseases will be discussed. NMR spectroscopy has been one of the most common platforms for metabolomic analysis in human infectious diseases caused by viruses [78–80]. The metabolomics research has been mainly based on comparisons and identification of differences between metabolic profiles

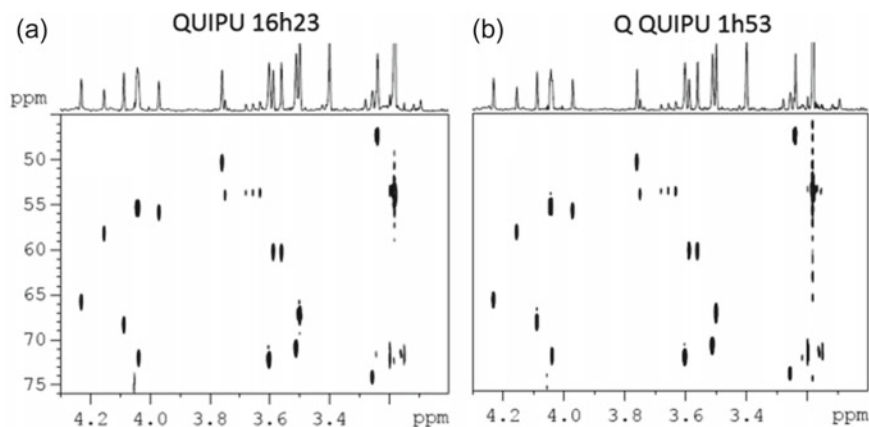


Fig. 9 2D maps of the methylene/methane area for a metabolite model mixture in ~ 16 h **a** using QUIPU and in less than 2 h **b** using Q QUIPU with 25% NUS and VRT function vd3. Reprinted (adapted) with permission from [63]. Copyright 2018 American Chemical Society

of study and control groups, such as the comparison of healthy and diseased individuals. Therefore, the objective of untargeted metabolomics in viral studies is to observe metabolic alterations associated with specific factors under study, aiming the discovery of diagnostic and prognostic biomarkers, and disease staging of viral infections. Metabolomics has been more employed in the past years for several viral infections as shown in Fig. 10. Here, we will focus primarily on those viruses in which a greater number of NMR-based metabolomics studies in patients with viral infections. Viral hepatitis B (HBV) [81], C (HCV) [82–88] and E (HEV) types [89], and human immunodeficiency virus (HIV) [90–96], are the most studied, as well as the response to many other viruses, such as West Nile virus [97], H1N1 influenza virus [98, 99], dengue virus [100] and other [101–103]. However, the COVID-19 pandemic disrupted this scenario, the metabolic profiles from patients with viral infection due to severe acute respiratory syndrome coronavirus 2 (SARS-CoV-2) have also been researched [51, 104–111]. The main works within the theme are listed in Table 3 which point to relevant remarks.

Most of NMR based metabolomics viral studies demonstrated high-level discrimination between the group of individuals with viral infection analyzed and the group of individuals not carrying viral infection analyzed or with a difference between the groups of individuals analyzed. These studies showed that metabolites present in plasma, urine, and to a lesser extent in saliva are differentially produced in response to HIV infection. In general, dysregulated metabolic pathways of patients caused by viral infection were also identified, such as TCA cycle, glycolysis, glutaminolysis, pentose phosphate pathway (PPP), fatty acid (FA) and lipid biosynthesis, β -oxidation, respiratory cycle (electron transport chain, ETC), and nucleotide and amino acid metabolism (Fig. 11).

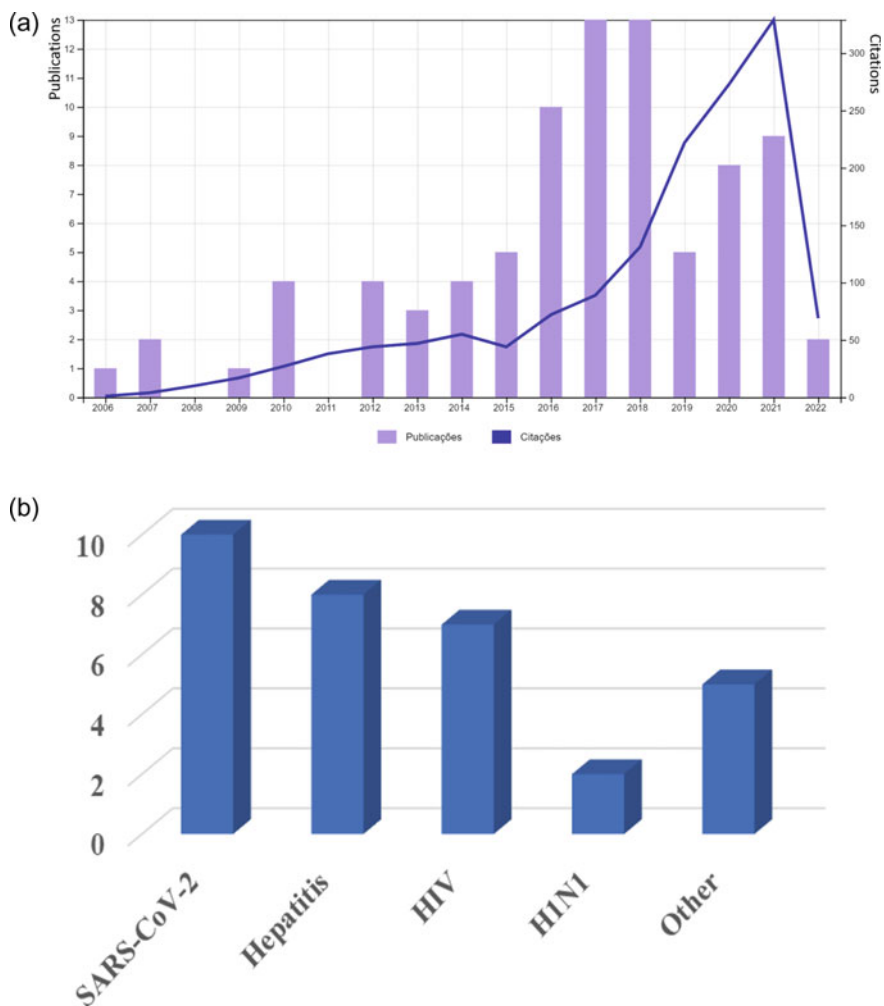


Fig. 10 **a** Trend in the virus NMR metabolomics publications and citations obtained using the keywords NMR metabolomics virus from the web of knowledge (<http://apps.webofknowledge.com>). **b** Number of scientific articles on NMR-based metabolomics studies of patients with infectious diseases caused by different viruses

The metabolism of viral studies is based on metabolites findings. The common metabolite NMR assignments are as follows in Table 4.

Table 3 Relevant remarks of NMR-based metabolomic studies of patients with infectious diseases caused by a virus

Virus	Sample	patients and/or individuals	Relevant remarks	References
HBV	Serum	HBV-liver cirrhosis (LC) HBV Healthy individuals (HI)*	Serum histidine as a potential biomarker for HBV patients Acetate, formate, pyruvate, and glutamine as potential biomarkers for progressing from HBV to HBV-LC Phenylalanine, unsaturated lipid, <i>n</i> -acetylglycoprotein, and acetone in the serum could be considered as a potential common biomarkers panel for these patients	Zheng et al. [81]
HBV and HCV	Urine	HCV HBV	Differentiating between the HCV and HBV patients The metabolites responsible by difference no were revealed	Godoy et al. [82]
HBV and HCV	Serum	HCV-fibrosis HCV-no fibrosis	Biologic pathways altered, mainly energetic metabolism involving glutamine/glutamate, carbohydrates, ketone bodies, and lipids Serum glucose is upregulated in HCV-fibrosis patients Acetoacetate at lower levels in HCV-fibrosis 3-hydroxybutyrate is downregulated in cirrhotic patients Serum creatine and creatinine at significantly lower levels in HCV-fibrosis	Embade et al. [112]

(continued)

3.1 Metabolomics Analysis in Severe Acute Respiratory Syndrome Coronavirus 2 (SARS-CoV-2) Infection

Coronavirus disease (COVID-19) is an infectious disease caused by severe acute respiratory coronavirus type 2 (SARS-CoV-2). Molecularly, severe COVID-9 disease is characterized by uncontrolled inflammatory syndrome caused by immune system

Table 3 (continued)

Virus	Sample	patients and/or individuals	Relevant remarks	References
HBV and HCV	Serum	HBV or HCV with schistosomiasis mansoni HBV or HCV monoinfected	Lactate and HDL are responsible for discrimination between the groups of patients Lactate at higher levels in coinfecting patients in comparison to mono-infected HDL at lower levels in coinfecting patients in comparison to mono-infected	Gouveia et al. [85]
HBV and HCV	Serum	HCV-before DAAs treatment HCV-after DAAs treatment Naïve HBV Healthy individuals	Distinction between the metabolomic profile of HCV patients before and after effective DAA treatment Tyrosine and formate at higher levels and potential biomarkers for the severity of HCV 3-hydroxybutyrate, formate, and acetate levels were significantly higher before DAAs therapy in HCV patients 2-oxoglutarate and 3-hydroxybutyrate at high levels in HCV patients when compared to HC and HBV individuals	Meoni et al. [86]
HCV	Serum	HCV (patients with different liver disease severity) Healthy individuals	Choline and histidine at high levels in HCV patients with late-stage of fibrosis when compared to early-stage fibrosis HCV individuals Choline/uric acid ration as a potential biomarker for differentiation of liver disease severity Serum 5-oxo-proline at higher levels in HCV in comparison to non-HCV individuals	Shanmuganathan et al. [87]

(continued)

Table 3 (continued)

Virus	Sample	patients and/or individuals	Relevant remarks	References
HEV	Serum and urine	HEV HBC Healthy individuals	L-isoleucine, acetone, and glycerol at reduced levels, while glycine at higher levels in the plasma in HEV patients Imidazole, 3-aminoisobutanoic acid, 1-methyl nicotinamide, bioppterin, adenosine, 1-methylhistidine, and salicyluric acid at lower levels on the urinary fluid in HEV patients Both HEV and HBV, 1-proline at high levels on the plasma and urinary when compared to HI	Munshi et al. [89]
HIV	Serum	HIV/AIDS-antiretroviral therapy; HIV/AIDS-no antiretroviral therapy HIV—negative (healthy individuals)	Discrimination between three analyzed groups	Hewer et al. [90]
HIV	Plasma	HIV/AIDS-antiretroviral therapy; HIV/AIDS-naïve therapy HIV-negative (healthy individuals)	Multivariate statistical analyzes unraveled distinct metabolic phenotypes and pathways among groups Glycolysis, TCA cycle, amino acid metabolism altered of the HIV/AIDS children	Kaur et al. [91]
HIV	Serum	HIV/AIDS-antiretroviral therapy; HIV/AIDS-naïve therapy; HIV-negative (healthy individuals)	Serum alanine at higher levels in HCV-negative, when compared to individuals with infection caused by HIV Alanine, glutamine, valine, taurine, and glucose levels can be altered due to viral infection and/or during antiretroviral therapy Alanine levels decrease, while glutamine and glucose increase with disease severity	McKnight et al. [92]

(continued)

Table 3 (continued)

Virus	Sample	patients and/or individuals	Relevant remarks	References
HIV	Serum	HIV/AIDS-antiretroviral therapy; HIV/AIDS-naïve therapy HIV-negative (healthy individuals)	Lipids, including low-density lipoprotein (LDL) and very-low-density lipoprotein (VLDL) mainly responsible for discrimination between infected individuals and HIV-negative	Philippeos et al. [93]
HIV	Serum	HIV/AIDS-antiretroviral therapy; HIV/AIDS-naïve therapy HIV-negative (healthy individuals)	Significant differences in glucose, lipids, phenylalanine, glutamic acid, aspartic acid, and branched amino acids compounds Aspartic acid, phenylalanine, and glutamic acid up-regulated in HIV individuals when compared to HIV-negative Tryptophan and tyrosine at lower levels in HIV-naïve therapy as compared to other groups Cystine at higher levels in HIV-naïve therapy as compared to other groups 11 metabolic pathways to be significantly altered by infection and/or treatment	Sitole et al. [95]

(continued)

hyperactivation. According to the World Health Organization (WHO), the standard method for diagnosis of acute SARS-CoV-2 infections is based on the detection of unique viral sequences by nucleic acid amplification tests (NAATs), such as rRT-PCR, however other methods are also used as microscopy, culture, antigen tests and antibody tests [120]. In this sense, intense efforts have been put into research on the application of single and multi-omics-based strategies have been carried out on several fronts to dissect a plethora of aspects involved in the SARS-CoV-2 infection. The understanding of the molecular processes altered by viral infection due to targeting host-response, providing the discovery of diagnostic and prognostic biomarkers for infectious diseases caused by SARS-CoV-2. However, the broad spectrum of severity of the COVID-19, and unpredictability in the outcome of the viral infection outcome make the metabolomic study of patients particularly challenging. Since the host response can be highly variable, the application of metabolomics

Table 3 (continued)

Virus	Sample	patients and/or individuals	Relevant remarks	References
HIV	Plasma, saliva, and urine	HIV/AIDS-antiretroviral therapy; HIV/AIDS-naïve therapy HIV-negative (healthy individuals)	Plasma and urine biofluids proportion better discrimination between HIV-infected individuals and HIV-negative than saliva Neopterin from urinary can be potential biomarkers for HIV-positive individuals Choline and sarcosine from serum can be potential biomarkers for HIV-positive individuals Serum sarcosine, Methylmalonic acid, D-Glucose, Choline, and L-Aspartic acid at high levels in HIV-infected individuals, when compared to HIV-negative individuals Metabolic pathways, such as metabolic cycles, glucose metabolism, hormone biosynthesis and amino acid biosynthesis pathways to be significantly altered by infection and/or treatment	Munshi et. al. [96]
HIV	Plasma		In HIV-infected individuals, atherogenic profile in terms of lipid and lipoprotein compositions and functions Classification of HIV-dyslipidemia from HIV normolipidemic VLDL particles, lactate, and LDL-TG compounds as potential biomarkers of dyslipidemia in patients on stable NNRTI-based ART and HIV-dyslipidemia predisposition	Rodriguez-Gallego et al. [94]

(continued)

Table 3 (continued)

Virus	Sample	patients and/or individuals	Relevant remarks	References
SARS-CoV-2	Plasma	COVID-19-hospitalized patients Healthy controls COVID-19-nonhospitalized patients (3 and 6 months pos-covid)	Tyrosine and formate at higher levels and potential In vitro diagnostics research (IVDr) protocol COVID-19 biomarker signatures in many Pos-COVID-19 patients At the elevated level the taurine, and reduced glutamine/glutamate ratio in Pos-COVID-19 patients in comparison to healthy controls Glutamate at an elevated level, glutamine at a reduced level, and a low glutamine/glutamate ratio in COVID-19 hospitalized patients in comparison to Pos-COVID-19 patients Glyc A and Kynurenine/tryptophan ration at elevated levels in Pos-COVID-19 patients, when compared to healthy individuals The HDL parameters H4A1, H4A2 (apolipoproteins A1 and A2 in HDL subfraction 4), and kynurenine were partially normalized in Pos-COVID patients Glyc A and Glyc B at higher levels in COVID-19-hospitalized patients, when compared to among groups	Holmes et al. [107]

(continued)

in COVID-19 becomes a major challenge in potential biomarkers for its diagnosis [121–123].

The metabolomics profile of COVID-9 patients has displayed dyslipidemia at every level of complexity [53]. Remarkably, the works have described rich lipoprotein information from plasma samples obtained by NMR spectroscopy, and several are using in vitro diagnostic research (IVDr) information on quantitative lipoprotein profiles [53, 104, 107–109]. In the studies described by Günther and collaborators [53], the NMR-based metabolomics experiments were conducted by the Bruker

Table 3 (continued)

Virus	Sample	patients and/or individuals	Relevant remarks	References
SARS-CoV-2	Plasma	COVID-19; Healthy controls	In vitro diagnostics research (IVDr) protocol 116 metabolic variables derived from NMR spectroscopy and 41 from mass spectrometry α -1-acid glycoprotein signal A (Glyc A) at elevated levels and an increased kynurenine/tryptophan ratio were discriminant metabolites between groups and inflammation markers Higher level of VLDL class parameters and a high Apolipoprotein B100/A1 ratio in COVID-19 patients Major HDL class particles and components at lower levels in COVID-19 patients Elevated glutamine/glutamate ratio as marked for liver dysfunction	Kimhofer et al. [108]

(continued)

in-vitro Diagnostic Research (IVDr) protocol, aiming to distinguish the metabolic profile between COVID-9 patients and healthy individuals. From the spectra collected using a pulse program noesygppr1d and cpmgpr1d, 39 metabolites and 112 lipoproteins were found by slash Instant 20% using Bruker Quantification in plasma/serum B.I Quant-Ps 2.0.0 and Bruker IVDr Lipoprotein Subclass Analysis B.I-Lisa (Bruker BioSpin). The study of individuals with severe SARS-CoV-2 hospitalized in an intensive care unit (ICU) exhibited a distinct serum metabolic profile when compared to healthy individuals. Metabolic differences were also found between COVID-19 patients and patients also submitted to ICU with respiratory distress as a consequence of cardiogenic shock. The lipoprotein profile investigated has whether showed severely altered in the COVID-19 patients about among analyzed groups, which signature to predict the severity of COVID-19 infection. When compared with healthy individuals, the individuals with COVID-19 prominently displayed dyslipidemia: Very-low-density lipoprotein and intermediate-density lipoprotein and associated apolipoprotein B and intermediate-density lipoprotein cholesterol; as well as the VLDL, IDL, and large-sized low-density lipoprotein (LDL)-1 particles were

Table 3 (continued)

Virus	Sample	patients and/or individuals	Relevant remarks	References
SARS-CoV-2	Plasma	COVID-19 Healthy controls Patients with Influenza-like and SARS-CoV-2 negative	In vitro diagnostics research (IVDr) protocol Glucose and α -1-acid glycoprotein are responsible for discrimination between the COVID-19 and healthy individuals Glyc A and Glyc B at higher levels in COVID-19 in comparison to Influenza-like (SARS-CoV-2) groups Alanine, lactate, and pyruvate at higher concentrations in COVID-19 than healthy controls · LDL cholesterol (LDCH), LDL phospholipids (LDPL), LDL-free cholesterol (LDFC), LDL apolipoprotein B, HDL cholesterol (HDCH), and phospholipids (HDPL) in higher levels in the healthy individuals VLDL cholesterol (e.g., V1CH, V2CH, and so forth) and triglycerides (e.g., V1TG, V2TG, and so forth) subclasses in higher levels in the COVID-19 individuals	Lodge et al. [51]

(continued)

increased, and triglycerides for nearly all lipoprotein subfractions. However, cholesterol and apolipoprotein A2 were decreased. In general, a severely disturbed lipoprotein profile with remarkably increased TG levels potentially contributes to atherosclerosis. Another important aspect addressed in the studies was demonstrating metabolic and lipoprotein profiles from asymptomatic individuals infected with SARS-CoV-2 were similar to healthy individuals absent antibody-negative [53].

The analyses and quantification of routine lipids, lipoprotein subclasses, fatty acids, and their saturation, as well as the low-molecular-weight metabolites, have been shown to play a relevant role in the metabolomic studies of the patients with SAR-CoV-2 [109, 110]. According to Izquierdo-Garcia et al. [111], the disease severity of the COVID-19 patients may be associated with serum 56 metabolites ($p < 0.05$), being mainly lipid and lipoprotein subclasses. Notably, increased triglyceride

Table 3 (continued)

Virus	Sample	patients and/or individuals	Relevant remarks	References
SARS-CoV-2	Plasma	COVID-19- ICU patients Healthy controls Pneumonia (negative SARS-CoV-2) patients	<ul style="list-style-type: none"> • 162 metabolites analyzed by DI-LC-MS/MS and NMR • Creatinine alone and creatinine/arginine ratio predicted ICU mortality with 100% accuracy • Kynurenine, arginine, and creatinine as potential biomarkers for diagnostic and prognostic for COVID-19 patients, as well as for patients stratification Lysophosphatidylcholines (LysoPCs) also helped discriminate between COVID19 patients and healthy individuals	Fraser et al. [105]
SARS-CoV	Serum	COVID-19	<ul style="list-style-type: none"> • In vitro diagnostics research (IVDr) protocol • Apolipoproteins, both Apo-A1 and Apo-A2, at lower levels in COVID-19 patients • Triglyceride (TG)-rich lipoprotein profile in the serum COVID-19 patient • TG-VLDL, TG-IDL, TG-LDL, and TG-HDL at higher levels in COVID-19 patients • TC-LDL and TC-HDL at lower levels in COVID-19 patients • Acetoacetic acid, 3-hydroxybutyric acid, and acetone were at markedly elevated levels in COVID-19 patients 	Bruzzone et al. [104]

(continued)

Table 3 (continued)

Virus	Sample	patients and/or individuals	Relevant remarks	References
SARS-CoV-2	Serum	COVID-19 patients in ICU Healthy individuals (control group) Patients in ICU caused by Cardiogenic shock Asymptomatic SARS-CoV-2 infection	<ul style="list-style-type: none"> • 39 metabolites and 112 lipoprotein-related parameters determined • In-vitro Diagnostic Research (IVDr) protocol • COVID-19 disease is associated with dyslipidemia • SARS-CoV-2 asymptomatic individuals did not develop dyslipidemia • Very-low-density lipoprotein (VLDL) and intermediate-density lipoprotein particles and associated apolipoprotein B and intermediate-density lipoprotein cholesterol at lower levels in COVID-19 patients • Glucose and formic acid at higher levels in COVID-19 patients, when compared to healthy individuals • Lactic acid and the lactic acid/pyruvic acid ratio were decreased in COVID-19 patients when compared to healthy individuals Creatine, creatinine, and phenylalanine at higher levels in COVID-19 suggesting alterations in hepatic or renal metabolism	Schmelter et al. [109]

(continued)

content and very-low-density lipoprotein (VLDL), a decrease in HDL, percentage of cholesterol/cholesteryl esters in HDL and IDL were associated with increased severity of COVID-19 disease. Furthermore, the acetoacetate, 3-hydroxybutyrate, phenylalanine metabolites, as well as the ratio of apolipoprotein B/apolipoprotein A were also biomarkers for the severity of COVID-19 patients.

An assessment of serum metabolites from SAR-CoV-2 patients has indicated a disturbed energy status [109]. The glucose and formic acid levels were increased, and the lactic acid/pyruvic acid ratio decreased compared to healthy individuals. These

Table 3 (continued)

Virus	Sample	patients and/or individuals	Relevant remarks	References
SARS-CoV-2	Plasma	COVID-19 COVID-19-tocilizumab treatment	Changes in the lipoprotein particles levels and composition associated with severe disease <ul style="list-style-type: none"> – Triglyceride content and VLDL at higher levels; a decrease in HDL – The percentage of cholesterol/cholesteryl esters in HDL, and IDL Acetoacetate, 3-hydroxybutyrate, phenylalanine, and the ratio of apolipoprotein B to A1 (ApoB/ApoA1) can be potential biomarkers for COVID-19 severity Valine levels, triglyceride content of VLDL, and the ratio of the polyunsaturated fatty acids (PUFA) were associated with tocilizumab treatment	Rendeiro et al. [110]
SARS-CoV-2	Serum	COVID-19 Influenza A	Free fatty acids, acetone, creatinine, and lactate at higher levels in COVID-19 Valine, 2-hydroxybutyrate, proline, methyl-guanidine, glucose, and tyrosine at higher levels in COVID-19 Branched-chain amino acids (isoleucine and valine) at higher levels in COVID-19 in comparison with Influenza A patients Lactate-to-glucose ratio can be a potential biomarker for the up-regulation of the glycolysis pathway in COVID-19 patients	Lorente et al. [111]

(continued)

Table 3 (continued)

Virus	Sample	patients and/or individuals	Relevant remarks	References
SARS-CoV-2	Plasma	COVID-19 (survivors) COVID-19 (patients with a worsening condition during the sampling period)	Metabolites described as the most important in the discrimination, not be specific to COVID-19 disease, since associated with inflammation, immune response, and energy metabolism 3-hydroxybutyrate, a ketone bodies representative at higher levels in COVID-19 patients BCAAs (branched-chain amino acids), including leucine and isoleucine at levels similar in both groups of patients Citrate at a lower level in the blood plasma in COVID-19 patients, suggesting changes in the TCA cycle	Baranovicoa et al. [113]

Healthy individuals (HI)* was a term used to describe individuals no-infected with the virus under study; HBV-liver cirrhosis (HBV-LC); direct-acting antiviral agents (DAAs), which are used in the treatment of hepatitis C; Acquired immune deficiency syndrome (AIDS); intensive care unit (ICU); severe acute respiratory syndrome coronavirus 2 (SARS-CoV-2); triglyceride (TG); cholesterol (TC); tricarboxylic acid (TCA) cycle; Very low-density lipoproteins (VLDL), intermediate-density lipoproteins (IDL); low-density lipoproteins (LDL); high-density lipoproteins (HDL); α -1-acid glycoprotein signal A (Gly A); α -1-acid glycoprotein signal B (Gly B) Lysophosphatidylcholines (LysoPCs)

studies identified a decrease in the alanine, glutamine and histidine may be associated with disrupted hepatic amino acid metabolism and hepatic damage. The hepatic or renal metabolism changes were also suggested by increased levels of creatine, creatinine, and phenylalanine in comparison to healthy individuals. Correia et al. also corroborated with this data showing that metabolomics from samples of COVID-19 patients is a powerful tool for a better understanding of the SARS-CoV-2 mechanism of action and metabolic consequences of the infection in the human body. They showed Glycerol, 3-aminoisobutyrate, formate, and glucuronate levels as alternated in COVID-19 patients, affecting the lactate, phenylalanine, tyrosine, and tryptophan biosynthesis, D-glutamine, D-glutamate, and glycerolipid metabolisms. Thus, SARS-CoV-2 infection presents disturbance in the energetic system, supporting the viral replication and corroborating with the severe clinical condition of the patient [124].

Another NMR-based metabolic approach that has been employed is the differential between COVID-19 patients and individuals that developed severe acute respiratory distress syndrome caused by the H1N1 influenza A virus [111]. In studies

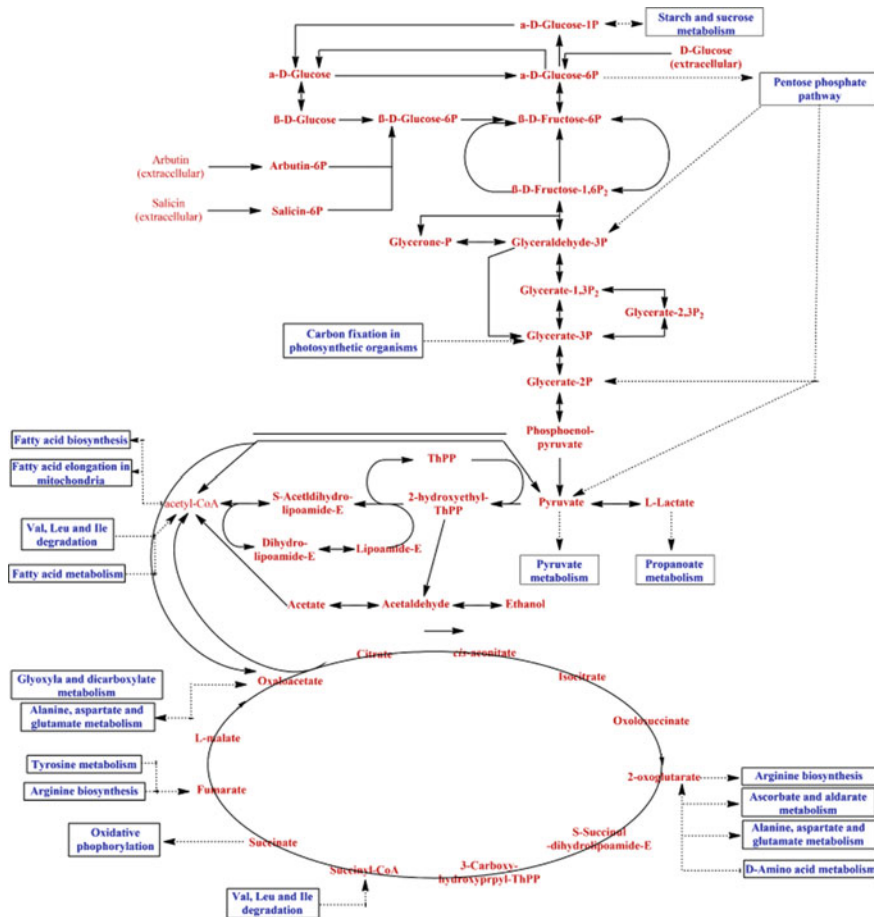


Fig. 11 Dysregulated metabolic pathways of patients caused by viral infections [114]

performed by Izquierdo-Garcia et al., the samples were analyzed by high-resolution magic angle spinning (HR-MAS-NMR), aiming to reduce the linewidth of the NMR due to macromolecules, such as proteins and lipids. HR-MAS reduces the line width of NMR spectra by spinning at a magic angle to a magic angle (54.7°) about the magnetic field. Serum samples of patients with viral infection in the intensive care unit (ICU) were analyzed by HR-MAS NMR at 4 °C to minimize metabolic degradation. From 1H spectra, the metabolites were identified by the Chenomx Profiler tool. Statical modeling of NMR data provided discrimination between the COVID-19 and H1N1 patients. The ICU patients due COVID-19 showed up-regulation of energy-generating pathways, such as glycolysis, fatty acid degradation, CoA biosynthesis, glycerolipids, and glycerophospholipids metabolism. A potential biomarker described for up-regulation in the glycolysis pathway of patients with SAR-CoV-2 infection was increased lactate/glucose ratio, when compared to patients with

Table 4 ^1H NMR assignment of common metabolites finding in biofluids [113, 115–119]

Metabolites	Chemical shift (ppm), multiplicity, integrals	Biofluid
Lipids and Lipoproteins		
Lipoprotein	0.82–0.93 (m), 1.20–1.37 (m)	Blood
Alcohols and derivatives		
Ethanol	1.17 (t; 3H) 3.65 (q; 2H)	Blood
Amines and derivatives		
Dimethylamine	2.50 (s; 6H)	Urine
Trimethylamine	2.88 (s; 9H)	Urine
Trimethylamine-N-oxide	3.25 (s; 9H)	Blood, Urine
Urea	5.78 (s; 4H)	Urine
Amino acids and derivatives		
1-Methylhistidine	3.06 (dd; 1H), 3.16 (dd; 1H), 3.69 (s; 3H), 3.96 (t; 1H), 6.99 (s; 1H), 7.89 (s; 1H)	Urine
2-Aminobutyric acid	1.18 (d; 3H), 2.59 (m; 1H), 3.02 (dd; 1H), 3.10 (dd; 1H)	Blood
2-Furoylglycine	3.92 (s; 2H), 6.62 (dd; 1H), 7.20 (dd; 1H), 7.85 (dd; 1H)	Urine
Alanine	1.47 (d; 3H), 3.78 (q; 1H)	Blood, urine
Arginine	1.53 (m; 1H), 1.59 (m; 1H), 1.86 (td; 2H), 3.17 (t; 2H), 3.77 (t; 1H)	Urine
Asparagine	2.84 (dd; 2H) 3.84 (t; 1H)	Blood
Betaine	3.89 (s; 2H), 3.25 (s; 9H)	Urine
Creatine	3.02 (s; 3H) 3.92 (s; 2H)	Blood, urine
Creatinine	3.03 (s; 3H) 4.04 (d; 1H) 4.09 (d; 1H)	Blood, urine
Glutamic acid	2.04 (m; 2H), 2.13 (m; 2H), 3.35 (m; 1H), 3.75 (m)	Blood
Glutamine	2.12 (td; 2H) 2.42 (dt; 1H) 2.46 (dt; 1H) 3.76 (t; 1H)	Blood
Glycine	3.55 (s; 2H)	Blood, urine
Guanidinoacetic acid	3.75 (s; 2H)	Urine
Histidine	3.15 (dd; 1H) 3.24 (dd; 1H) 3.98 (t; 1H) 7.07 (s, 1H) 7.82 (s; 1H)	Blood, urine
Isoleucine	0.92 (t; 3H) 1.00 (d; 2H) 1.00 (d; 1H) 1.25 (m; 2H) 1.97 (m; 1H) 3.66 (t; 3H)	Blood
Leucine	0.94 (d; 3H), 0.96 (d; 3H), 1.71 (m; 3H); 3.73 (dd; 1H)	Blood
Lysine	1.43 (m; 2H) 1.72 (tt; 2H) 1.90 (dtd; 1H) 2.12 (dtd; 1H) 3.01 (t; 1H) 3.74 (t; 1H)	Blood

(continued)

Table 4 (continued)

Metabolites	Chemical shift (ppm), multiplicity, integrals	Biofluid
Methionine	2.11 (dtd; 1H) 2.12 (s; 3H) 2.19 (dtd; 1H) 2.63 (t;2H) 3.85 (t; 1H)	Blood, urine
Dimethylglycine	2.92 (s; 6H), 3.72 (s; 2H)	Blood, urine
Ornithine	1.78 (tt; 2H) 1.94 (td; 1H) 3.04 (t; 2H) 3.74 (t; 1H)	Blood
Phenylalanine	3.12 (m; 1H), 3.28 (m; 1H), 3.99 (dd; 2H), 7.32 (d; 2H), 7.40 (t; 1H), 7.42 (t; 2H)	Blood
Proline	1.47 (m;1H) 1.75 (m; 2H) 2.20 (m; 1H) 2.99 (ddd; 1H) 3.40 (ddd; 1H) 3.57 (dd; 1H)	Blood
Sarcosine	2.73 (s; 3H) 3.60 (d; 1H) 3.78 (d; 1H)	Blood, urine
Taurine	3.25 (t;2H), 3.41 (t;2H)	Urine
Threonine	1.32 (d; 3H), 3.58 (d; 1H), 4.25 (m; 1H)	Blood
Tryptophan	7.19 (t; 1H), 7.28 (t; 1H), 7.32 (s; 1H), 7.54 (d; 1H), 7.73 (d;1H)	Blood
Tyrosine	6.88 (d; 2H), 7.18 (d; 2H)	Blood
Valine	0.97 (d; 3H), 1.03 (d; 3H), 2.25 (m; 1H), 3.59 (d; 1H)	Blood, urine
Benzene and substituted derivatives		
Benzoic acid	7.47 (dd; 2H), 7.54 (t; 1H), 7.86 (d; 2H),	Urine
Mandelic acid	4.93 (s, 1H), 7.13 (m, 1H), 7.41 (tt, 1H), 7.44 (m, 1H), 7.45 (m, 1H)	Urine
Hippuric acid	3.96 (d, 2H), 7.54 (m, 2H), 7.63 (tt, 1H), 7.83 (dd, 2H)	Urine
Carboxylic acids		
2-Hydroxybutyric acid	0.89 (t; 3H) 1.64 (m; 2H) 3.98 (t; 1H)	Blood
Acetic acid	1.91 (s; 3H)	Blood, urine
Citric acid	2.52 (d; 2H), 2.68 (d; 2H)	Blood, urine
Formic acid	8.45 (s; 1H)	Blood, urine
Fumaric acid	6.38 (s;2H)	Urine
Imidazole	7.26 (s; 3H)	Urine
Lactic acid	1.32 (d; 3H), 4.10 (q; 1H)	Blood, urine
Proline betaine	3.57(s;1H), 3.31 (s; 2H), 3.26 (s; 6H), 2.58 (s; 2H), 2.02 (s; 2H)	Urine
Succinic acid	2.39 (t; 4H)	Blood, urine
Tartaric acid	3.70 (d; 1H), 4.34 (d; 1H)	Urine

(continued)

Table 4 (continued)

Metabolites	Chemical shift (ppm), multiplicity, integrals	Biofluid
Trignolline	4.33 (s; 3H), 8.07 (m; 1H), 8.83 (m; 2H), 9.11 (s; 1H),	Urine
Fatty acids and derivatives		
2-Methylsuccinic acid	1.09 (m; 3H), 2.12 (dd; 1H), 2.51 (dd; 1H), 2.61 (td; 1H),	Urine
Essential nutrient		
Choline	3.19 (s; 6H) 3.50 (m; 2H) 4.10 (s; 2H)	Blood
Keto acids and derivatives		
2-Oxoglutaric acid		Blood, urine
3-Hydroxybutyric acid	1.19 (d; 2H) 2.29 (dd; 1H) 2.39 (dd; 1H) 4.14 (td; 1H)	Blood, urine
Acetoacetic acid	2.27 (s; 3H) 3.43 (s; 2 H)	Blood, urine
Acetone	2.22 (s; 6H)	Blood, urine
Oxaloacetic acid	3.32 (s; 2H)	Urine
Pyruvic acid	2.37 (s; 3H)	Blood, urine
Purine, Pyridine, and Pyrimidine derivatives		
1-Methyladenosine	3.49 (dd; 1H), 3.75 (dd; 2H), 3.97 (s; 3H), 4.12 (td; 1H), 4.68 (dd; 1H), 5.90 (d; 1H), 8.28 (s; 1H), 8.31 (s; 1H)	Urine
1-Methylnicotinamide	4.47 (s; 3H), 8.18 (t; 1H), 8.89 (d; 1H), 8.96 (d; 1H), 9.28 (d; 1H)	Urine
Adenosine	3.49 (td; 1H), 3.49 (dd; 1H), 3.75 (dd; 1H), 3.91 (dd; 1H), 4.62 (d; 1H), 4.73 (dd; 1H), 8.49 (s; 2H)	Urine
Allatoin	4.12 (s; 1H)	Urine
Allopurinol	7.51 (s; 1H), 8.01 (s; 1H)	Urine
Caffeic acid	6.33 (d; 1H), 6.92 (d; 1H), 7.06 (dd; 1H), 7.14 (d; 1H), 7.29 (d; 1H)	Urine
Inosine	3.86 (dd; 1H), 3.93 (dd; 1H), 4.34 (dd; 1H), 4.38 (td; 1H), 4.78 (dd; 1H), 6.09 (d; 1H), 8.49 (s; 2H)	Urine
Sugars and derivatives		
D-Galactose	3.71 (t; 1H) 3.71 (dd; 1H) 3.75 (quint; 2H) 3.81 (dd; 1H) 3.99 (d, 1H) 5.27 (d; 1H)	Blood, urine
D-Glucose	3.25 (m; 1H), 3.41 (m; 2H), 3.48 (m; 2H), 3.54 (dd; 1H), 3.72 (m; 3H), 3.76 (dd), 3.82 (m; 2H), 3.89 (dd; 1H), 4.65 (d; 1H), 5.23 (d; 1H)	Blood, urine

(continued)

Table 4 (continued)

Metabolites	Chemical shift (ppm), multiplicity, integrals	Biofluid
D-lactose	5.18 (s; H), 4.63 (s; H), 4.12 (s; H), 3.84 (s; H), 3.81 (s; H), 3.75 (s; H) 3.63 (s; H) 3.53 (s; H)	Urine
D-mannitol	3.61 (dd;1H) 3.71 (td;1H) 3.71 (dd;1H) 3.72 (td;1H) 3.83 (dd;1H) 3.84 (dd;1H) 3.88 (dd;1H)	Urine
D-mannose	3.47 (dt; 1H) 3.68 (dd; 1H) 3.75 (dd; 1H) 3.80 (dd; 1H) 3.82 (dd; 1H) 3.95 (dd; 1H) 5.21 (d; 1H)	Urine
Glucuronate	3.27 (m; 1H), 3.49 (m; 2H), 3.57 (dd; 1H), 3.71 (m; 1H), 4.05 (d; 1H), 4.65 (d; 2H), 5.23 (d; 1H)	Blood
Glycerol	3.55 (m; 4H), 3.64 (m; 4H), 3.78 (m; 1H)	Blood
Myo-Inositol	3.87 (t; 1H) 3.87 (dd; 2H) 4.12 (dd;2H) 4.12 (dd; 1H)	Urine
Sulfones		
Dimethylsulfone	3.14 (s; 6H)	Blood

influenza A. The decrease in the amino acid metabolism in COVID-19 patients is mainly due to isoleucine and valine at low levels. The branched-chain amino acids levels may be associated with intense inflammatory of host-response, the authors suggesting that the lower levels of BCAAs in COVID-19 patients may be indicative of less intense inflammatory response in patients infected with SARS-CoV-2 than influenza A patients [111].

The metabolomic data and immune response were used to develop the approach to stratification of COVID-19 patients. Through regularized Canonical Correlation Analysis (rCCA), both NMR and flow cytometry datasets were integrated, and six groups were characterized by distinct clinical parameters and an abundance of immune-metabolic species [110]. The groups characterized by mild COVID-19 patients were differentiated by distinct BMI, liver enzyme levels, and triglyceride content of lipoproteins. While stratifying between “late” and “earlier” severe COVID-19 patients, one of the main factors was creatinine level, being at a higher level in the late group than that the “earlier” severe group [110].

The response of COVID-19 patients to drug therapy is also being monitored by metabolic changes. Salvatore et al. reported a metabolomics study of ten COVID-19 patients hospitalized with hyper inflammation before and after treatment with Tocilizumab. The metabolic profile of the patients treated with Tocilizumab was more similar to patients with milder infection viral. However, the metabolites are associated with the severity of COVID-19 patients [110].

3.2 *Metabolomics Analysis in Hepatitis C Viral Infection*

Chronic hepatitis C virus infection can lead to progressive liver diseases, such as chronic liver disease, cirrhosis, and hepatocellular carcinoma [125, 126]. Similar to other forms of chronic liver disease, the progression of the viral infections caused by HCV is accompanied by liver fibrosis. The liver biopsy is the gold standard method for detecting liver disease and fibrosis through different semiquantitative and validated histological scores. The METAVIR system scores fibrosis on a scale ranging from 0 to 4, where F0 indicates the absence of fibrosis and F4 is a fully developed cirrhosis. There is currently an immense interest in the diagnosis and prognosis for hepatitis viruses in a non-invasive way. In this context, NMR-based metabolomics studies have been performed to identify potential biomarkers for HCV, as well as HBV and HEV, to effectively distinguish patients in different stages and healthy individuals [125–128].

The liver plays a central role in energy and lipid metabolism. Liver diseases affect lipids levels, including those caused by HCV, hepatitis B virus (HBV), and hepatitis E virus (HEV). Serum lipid profile can be a biomarker of liver insufficiency in fibrosis and cirrhosis patients [112]. According to Millet and collaborators [112], low-density lipids, such as VLDL and VLDL2, were found at higher levels in HCV-cirrhosis patients when compared to healthy individuals. The serum of patients with HBV and HBV-LC also exhibited a high concentration of unsaturated lipid in comparison to healthy individuals. On the other hand, the low-density lipoproteins (LDL) and lipoproteins with higher densities (HDL) were observed at lower levels in cirrhotic-HCV patients compared to HCV non-fibrotic patients [112]. In another study [83], the spectra profile of serum of HCC and HCV patients showed clear differences. From broad signals of the ^1H spectra, the fatty acid methyl and methylene moieties were determined, however, lipids with different fatty acid chains were not differentiated due to their overlapping signals [83].

Silva et al. also reported differences between coinfecting patients with schistosomiasis and HBV/HCV chronic infection and HBV/HCV chronic monoinfected patients regarding the levels of HDL and triglycerides. By conventional assays, these metabolites did not present any statistically significant in the different analyzed groups [94]. Similarly, Gao et al. [81] reported that HBV-LC and HBV patients had a higher level of saturated/monounsaturated fatty acid and a lower level of polyunsaturated fatty acid than healthy individuals.

Undoubtedly, in the different works reported in the literature, there is a great variation of several metabolites, mainly low molecular weight metabolites, between the groups of patients infected with the hepatitis virus. They are assigned to different metabolites, such as amino acids, organic acids, creatine, creatinine, and choline, among others. Since then, NMR-based metabolomic studies have demonstrated alterations in biological pathways of the patients with viral infection caused by hepatitis, mainly energetic metabolism involving glutamine/glutamate, carbohydrates, ketone bodies, and lipids. The distinction between analyzed groups is reported by comparing the concentrations of only a reduced set of metabolites [86, 87, 112].

A pilot study reported by Simas et al. in 2010 demonstrated the potential of NMR-based metabolomics on urine samples for differentiating patients infected with HCV from healthy individuals with sensitivity and specificity [82].

In the serum metabolite comparison of HBV, HBV-liver cirrhotic and healthy individuals, the histidine, *n*-acetylglycoprotein, phenylalanine, acetone, unsaturated lipid, and citrate were the main metabolites for differentiation of the analyzed groups [81]. Compared to HBV patients, serum phenylalanine and unsaturated lipid concentrations were higher in the serum of patients in the severe stage (HBV-LC), while that *n*-acetylglycoprotein and acetone were found at lower levels. To distinguish HBV patients from healthy individuals, the serum histidine and citrate were described as important metabolites that contributed to the distinction of these groups [81].

The differentiation between the metabolomics profile of individuals with hepatocellular carcinoma (HCC) from the Hepatitis C virus (HCV) population was achieved through OSP-PLS analysis of the NOESY spectra. Therefore, the contributions of lipids were most prominent, however, the lipids responsible for separation were not attributed. About low-molecular-weight metabolites, creatinine, valine, and choline were found at higher levels in HCC patients than in HCV. Choline is an important metabolite in several cancer types in high concentrations, which plays a key role in the synthesis of phospholipids for cancer cell membranes and donors in methylation reactions. The advanced stages of liver fibrosis/cirrhosis in both diseases, HCC and HCV, can lead to a higher concentration of this metabolite [83].

A cross-platform serum metabolomics study compared the performance of MSI-CE-MS and NMR methods standardized protocols [88]. Both platforms offered similar reproducibility with a good mutual agreement to classify HCV individuals in different stages of the disease. The researchers highlighted the NMR metabolomics approach by an automated spectral processing and deconvolution software, as well as the identification and quantification of metabolites by a serum-specific metabolite library. However, there are disadvantages of 1D NMR over MSI-CE-MS. MSI-CE-MS spectrometric was improved resolution and lower detection limits, as result, MSI-CE-MS, 60 serum metabolites were found in the HCV patient samples, while by NMR platform were determined 47 metabolites, being 30 serum metabolites were reliably determined in most non-HCV controls and HCV patients. In both instrumental platforms, serum choline and histidine metabolites were found as the best biomarkers to distinguish between HCV patients in late-stage fibrosis and early-stage fibrosis HCV individuals [88]. In other studies, choline is also one of the most significant biomarkers to assess liver cirrhosis in HCV individuals [112]. It is worth mentioning that several other serum metabolites were determined with increasing liver fibrosis, such as asparagine, arginine, tyrosine, and hydroxyproline [87].

Serum creatine and creatinine levels are also associated as biomarkers to differentiate HCV patients of different fibrosis stages [112]. These metabolites were found at higher levels in HCV patients in the non-fibrotic than HBV-LC patients. Creatine is an important metabolite in the energy transfer process, which is synthesized primarily in the liver and is again involved in the general energy supply [113].

Glucose is a metabolite with significant variations in its concentration in the serum of patients infected with hepatitis virus [85, 112]. As reported by Millet et al.

in NMR-based metabolomics [110], HCV-cirrhosis patients present a high level of serum glucose when compared to HCV-no cirrhosis individuals. Similarly, Embade et al. reported towards patients with mild or severe chronic liver in comparison to healthy individuals. The severity of liver diseases is also associated with glucose metabolism changes. The high level of serum glucose in severe cirrhosis patients may be related to reduced metabolism via the tricarboxylic acid cycle. Also, the upregulation of serum glucose is associated with a lower level of glycerol, which can be metabolized to glucose in the liver and result in energy for cellular metabolism [112].

4 Conclusions and Future Perspectives

Amongst the methodologies reported, communication efforts are required to make end-users aware of recent methodological advances. Otherwise, NMR method improvements may not cross laboratory doors to meet the outside world. Efforts to standardize the metabolomics protocols and solve pattern metabolomics issues allow the integration of international cooperation to determine the metabolism type of a wide range of viral diseases.

Acknowledgements Authors acknowledge the financial support from CAPES (Grant no. 88887.504531/2020-00, from notice no. 09/2020) and FAPESP (grant no. 17/01189-0). DRC acknowledge the continued support from CNPq Research Productivity Program (309212/2019-7).

References

1. World Health Organization, WHO Director-General's opening remarks at the media briefing on COVID-19. <https://www.who.int/director-general/speeches/detail/who-director-general-s-opening-remarks-at-the-media-briefing-on-covid-19---11-march-2020>
2. S. Crimi, L. Fiorillo, A. Bianchi et al., Herpes virus, oral clinical signs, and qol: systematic review of recent data. *Viruses* **11**, 1–18 (2019). <https://doi.org/10.3390/v11050463>
3. M.H. Ebell, Epstein-Barr virus infectious mononucleosis. *Am Fam Physician* **70** (2004)
4. T. Wilkins, J.K. Malcolm, D. Raina, R.R. Schade, Hepatitis C: diagnosis and treatment. *Am Fam Physician* **81**, 1351–1357 (2010)
5. World Health Organization, Yellow fever (2019). <https://www.who.int/news-room/fact-sheets/detail/yellow-fever#:~:text=Symptoms of yellow fever include, and Central and South America>
6. W.J. Wiersinga, A. Rhodes, A.C. Cheng et al., Pathophysiology, transmission, diagnosis, and treatment of coronavirus disease 2019 (COVID-19): a review. *JAMA* **324**, 782–793 (2020). <https://doi.org/10.1001/jama.2020.12839>
7. T. Hemachudha, G. Ugolini, S. Wacharapluesadee et al., Human rabies: neuropathogenesis, diagnosis, and management. *Lancet Neurol* **12**, 498–513 (2013). [https://doi.org/10.1016/S1474-4422\(13\)70038-3](https://doi.org/10.1016/S1474-4422(13)70038-3)
8. P. Davison, J. Morris, Mumps, in *StatPearls* (StatPearls Publishing, Treasure Island, 2022)

9. A. Misin, R.M. Antonello, S. Di Bella et al., Measles: an overview of a re-emerging disease in children and immunocompromised patients. *Microorganisms* **8**, 1–16 (2020). <https://doi.org/10.3390/microorganisms8020276>
10. World Health Organization, Influenza (2018). [https://www.who.int/news-room/fact-sheets/detail/influenza-\(seasonal\)](https://www.who.int/news-room/fact-sheets/detail/influenza-(seasonal))
11. World Health Organization, Dengue and severe dengue (2022). <https://www.who.int/news-room/fact-sheets/detail/dengue-and-severe-dengue>
12. A.R. Xavier, S. Kanaan, R.P. Bozzi, L.V. Amaral, Clinical and laboratory diagnosis of Zika fever: an update. *J Bras Patol e Med Lab* **53**, 252–257 (2017). <https://doi.org/10.5935/1676-2444.20170039>
13. World Health Organization, Ebola virus disease (2021). <https://www.who.int/news-room/fact-sheets/detail/ebola-virus-disease>
14. F. Ayoade, S. Kumar, Varicella zoster, in *StatPearls* (StatPearls Publishing, Treasure Island, 2022)
15. K.A. Simonsen, SJ Smallpox, in *StatPearls* (StatPearls Publishing, Treasure Island)
16. M. Truong Lam, B. O'Sullivan, P. Gullane, S.H. Huang, Challenges in establishing the diagnosis of human papillomavirus-related oropharyngeal carcinoma. *Laryngoscope* **126**, 2270–2275 (2016). <https://doi.org/10.1002/lary.25985>
17. S.U. Kalu, M. Loeffelholz, E. Beck, J.A. Patel, K. Revai, J. Fan, K.J. Henrickson, T. Chonmaître, Persistence of adenovirus nucleic acids in nasopharyngeal secretions: a diagnostic conundrum. *Bone* **29**, 746 (2010). <https://doi.org/10.1097/INF.0b013e3181d743c8>
18. World Health Organization, Hepatitis B (2021). <https://www.who.int/news-room/fact-sheets/detail/hepatitis-b>
19. C. Chu, P.A. Selwyn, Diagnosis and initial management of acute HIV infection. *Am Fam Physician* **81**, 1239–1244 (2010)
20. Centers of Disease Control and Prevention, Poliovirus diagnostic methods (2021). <https://www.cdc.gov/polio/what-is-polio/lab-testing/diagnostic.html>
21. G.L. Kirkpatrick, The common cold. *Prim Care Clin Off Pract* **23**, 657–675 (1996). [https://doi.org/10.1016/S0095-4543\(05\)70355-9](https://doi.org/10.1016/S0095-4543(05)70355-9)
22. B. Alberts, D. Bray, A. Johnson et al., *Fundamentos da Biologia Celular. Uma Introdução à Biologia Molecular da Célula*. Artes Médicas Sul, Porto Alegre (2006)
23. J.B. Reece et al., *Biologia de Campbell*, 10th edn. (Artmed, Porto Alegre, 2015)
24. C.B. Clish, Metabolomics: an emerging but powerful tool for precision medicine. *Mol Case Stud* **1**, a000588 (2015). <https://doi.org/10.1101/mcs.a000588>
25. S.Z. Tan, P. Begley, G. Mullard et al., Introduction to metabolomics and its applications in ophthalmology. *Eye* **30**, 773–783 (2016). <https://doi.org/10.1038/eye.2016.37>
26. R.G. Duft, A. Castro, M.P.T. Chacon-Mikahil, C.R. Cavaglieri, Metabolomics and exercise: possibilities and perspectives. *Mot Rev Educ Física* **23** (2017). <https://doi.org/10.1590/s1980-6574201700020010>
27. K.S. Smirnov, T.V. Maier, A. Walker et al., Challenges of metabolomics in human gut microbiota research. *Int J Med Microbiol* **306**, 266–279 (2016). <https://doi.org/10.1016/j.ijmm.2016.03.006>
28. A. Smolinska, L. Blanchet, L.M.C. Buydens, S.S. Wijmenga, NMR and pattern recognition methods in metabolomics: from data acquisition to biomarker discovery: a review. *Anal. Chim. Acta* **750**, 82–97 (2012). <https://doi.org/10.1016/j.aca.2012.05.049>
29. A. Marco-Ramell, M. Palau-Rodríguez, A. Alay et al., Evaluation and comparison of bioinformatic tools for the enrichment analysis of metabolomics data. *BMC Bioinformatics* **19**, 1–11 (2018). <https://doi.org/10.1186/s12859-017-2006-0>
30. C. Lema, M. Andrés, S. Aguadé-Bruix et al., ¹H NMR serum metabolomic profiling of patients at risk of cardiovascular diseases performing stress test. *Sci. Rep.* **10**, 1–10 (2020). <https://doi.org/10.1038/s41598-020-74880-6>
31. V. Pareek, H. Tian, N. Winograd, S.J. Benkovic, Metabolomics and mass spectrometry imaging reveal channeled de novo purine synthesis in cells. *Science* **368**, 283–290 (2020). <https://doi.org/10.1126/science.aaz6465>

32. D.D. Fraser, G. Cepinskas, E.K. Patterson et al., Novel outcome biomarkers identified with targeted proteomic analyses of plasma from critically ill coronavirus disease 2019 patients. *Crit. Care Explor.* **2**, e0189 (2020). <https://doi.org/10.1097/ccce.0000000000000189>
33. B.L. Marquez, R.T. Williamson, Quantitative applications of NMR spectroscopy. *Chem. Eng. Pharm. Ind.* 133–149 (2019). <https://doi.org/10.1002/9781119600800.ch7>
34. J.L. Ward, J.M. Baker, M.H. Beale, Recent applications of NMR spectroscopy in plant metabolomics. *FEBS J* **274**, 1126–1131 (2007). <https://doi.org/10.1111/j.1742-4658.2007.05675.x>
35. A.A. Crook, R. Powers, Quantitative NMR-based biomedical metabolomics: current status and applications. *Molecules* **25** (2020). <https://doi.org/10.3390/molecules25215128>
36. G.A. Nagana Gowda, D. Raftery, Overview of NMR Spectroscopy-Based Metabolomics: Opportunities and Challenges (2019), pp. 3–14
37. P. Soininen, in *Quantitative 1H NMR Spectroscopy—Chemical and Biological Applications* (2008)
38. C. Deborde, A. Moing, L. Roch et al., Plant metabolism as studied by NMR spectroscopy. *Prog. Nucl. Magn. Reson. Spectrosc.* **102–103**, 61–97 (2017). <https://doi.org/10.1016/j.pnmrs.2017.05.001>
39. A. Vignoli, V. Ghini, G. Meoni et al., High-throughput metabolomics by 1D NMR. *Angew. Chemie. Int. Ed.* **58**, 968–994 (2019). <https://doi.org/10.1002/anie.201804736>
40. M. Schmedes, A.D. Brejtnrod, E.K. Aadland et al., The effect of lean-seafood and non-seafood diets on fecal metabolites and gut microbiome: results from a randomized crossover intervention study. *Mol. Nutr. Food Res.* **63**, 1–8 (2019). <https://doi.org/10.1002/mnfr.201700976>
41. R. Thøgersen, J.L. Castro-Mejía, U. Kræmer Sundekilde et al., Inulin and milk mineral fortification of a pork sausage exhibits distinct effects on the microbiome and biochemical activity in the gut of healthy rats. *Food Chem.* **331** (2020). <https://doi.org/10.1016/j.foodchem.2020.127291>
42. P.S.X. Yap, C.W. Chong, A.A. Kamar et al., Neonatal intensive care unit (NICU) exposures exert a sustained influence on the progression of gut microbiota and metabolome in the first year of life. *Sci. Rep.* **11**(1353), 1 (2021). <https://doi.org/10.1038/s41598-020-80278-1>; *Sci. Rep.* **11**(1–14), 10 (2021). <https://doi.org/10.1038/s41598-021-88758-8>
43. X. Li, K. Hu, Quantitative NMR studies of multiple compound mixtures. *Annu. Reports NMR Spectrosc.* **90**, 85–143 (2017). <https://doi.org/10.1016/bs.armmr.2016.08.001>
44. P. Giraudeau, Challenges and perspectives in quantitative NMR. *Magn. Reson. Chem.* **55**, 61–69 (2017). <https://doi.org/10.1002/mrc.4475>
45. R.L. Loo, S. Lodge, T. Kimhofer et al., Quantitative in-vitro diagnostic NMR spectroscopy for lipoprotein and metabolite measurements in plasma and serum: recommendations for analytical artifact minimization with special reference to COVID-19/SARS-CoV-2 samples. *J. Proteome. Res.* **19**, 4428–4441 (2020). <https://doi.org/10.1021/acs.jproteome.0c00537>
46. M.P.M. Letertre, P. Giraudeau, P. de Tullio, Nuclear magnetic resonance spectroscopy in clinical metabolomics and personalized medicine: current challenges and perspectives. *Front. Mol. Biosci.* **8**, 1–25 (2021). <https://doi.org/10.3389/fmolb.2021.698337>
47. D.L. Pavia et al., Introduction to spectroscopy. Cengage Learn (2009)
48. T.D.W. Claridge, in *High-Resolution NMR Techniques in Organic Chemistry* (Elsevier, 2009)
49. C. Stavarache, A. Nicolescu, C. Duduianu et al., A real-life reproducibility assessment for NMR metabolomics. *Diagnostics* **12** (2022). <https://doi.org/10.3390/diagnostics12030559>
50. B. Jiménez, E. Holmes, C. Heude et al., Quantitative lipoprotein subclass and low molecular weight metabolite analysis in human serum and plasma by 1H NMR spectroscopy in a multi-laboratory trial. *Anal. Chem.* **90**, 11962–11971 (2018). <https://doi.org/10.1021/acs.analchem.8b02412>
51. S. Lodge, P. Nitschke, T. Kimhofer et al., NMR spectroscopic windows on the systemic effects of SARS-CoV-2 infection on plasma lipoproteins and metabolites in relation to circulating cytokines. *J. Proteome Res* **20**, 1382–1396 (2021). <https://doi.org/10.1021/acs.jproteome.0c00876>

52. R. Masuda, S. Lodge, P. Nitschke et al., Integrative modeling of plasma metabolic and lipoprotein biomarkers of SARS-CoV-2 infection in Spanish and Australian COVID-19 patient cohorts. *J. Proteome. Res.* **20**, 4139–4152 (2021). <https://doi.org/10.1021/acs.jproteome.1c00458>
53. S. Lodge, P. Nitschke, R.L. Loo et al., Low volume in vitro diagnostic proton NMR spectroscopy of human blood plasma for lipoprotein and metabolite analysis: application to SARS-CoV-2 biomarkers. *J. Proteome. Res.* **20**, 1415–1423 (2021). <https://doi.org/10.1021/acs.jproteome.0c00815>
54. G. Costa Dos Santos Junior, C.M. Pereira, T. Kelly Da Silva Fidalgo, A.P. Valente, Saliva NMR-based metabolomics in the war against COVID-19. *Anal. Chem.* **92**, 15688–15692 (2020). <https://doi.org/10.1021/acs.analchem.0c04679>
55. B. Khakimov, H.C.J. Hoefsloot, N. Mobaraki et al., Human blood lipoprotein predictions from 1H NMR spectra: protocol, model performances, and cage of covariance. *Anal. Chem.* **94**, 628–636 (2022). <https://doi.org/10.1021/acs.analchem.1c01654>
56. C. Wang, I. Timári, B. Zhang et al., COLMAR lipids web server and ultrahigh-resolution methods for two-dimensional nuclear magnetic resonance- and mass spectrometry-based lipidomics. *J. Proteome. Res.* **19**, 1674–1683 (2020). <https://doi.org/10.1021/acs.jproteome.9b00845>
57. B.S. Barbosa et al., Qualitative and quantitative NMR approaches in blood serum lipidomics, in *Investigations of Early Nutrition Effects on Long-Term Health* (Humana Press, New York, 2018), pp. 365–379
58. Y. Navarro, R. Soengas, M.J. Iglesias, F.L. Ortiz, Use of NMR for the analysis and quantification of the sugar composition in fresh and store-bought fruit juices. *J. Chem. Educ.* **97**, 831–837 (2020). <https://doi.org/10.1021/acs.jchemed.9b00651>
59. G.A.N. Gowda, D. Rafferty, NMR based metabolomics. 19–37 (2022). <https://doi.org/10.1007/978-3-030-51652-9>
60. Q. Wan, Y. Wang, H. Tang, Quantitative 13C traces of glucose fate in hepatitis B virus-infected hepatocytes. *Anal. Chem.* **89**, 3293–3299 (2017). <https://doi.org/10.1021/acs.analchem.6b03200>
61. A.L. Guennec, P. Giraudeau, S. Caldarelli, Evaluation of fast 2D NMR for metabolomics. *Anal. Chem.* **86**, 5946–5954 (2014). <https://doi.org/10.1021/ac500966e>
62. Maulidiani, F. Abas, R. Rudyanto et al., Application of quantitative spectral deconvolution 1H NMR (qsd-NMR) in the simultaneous quantitative determination of creatinine and metformin in human urine. *Anal. Methods* **11**, 5487–5499 (2019). <https://doi.org/10.1039/c9ay00594c>
63. J. Farjon, C. Milande, E. Martineau et al., The FAQUIRE approach: fast, quantitative, highly resolved and sensitivity enhanced 1H, 13C Data. *Anal. Chem.* **90**, 1845–1851 (2018). <https://doi.org/10.1021/acs.analchem.7b03874>
64. E. Martineau, J.N. Dumez, P. Giraudeau, Fast quantitative 2D NMR for metabolomics and lipidomics: a tutorial. *Magn. Reson. Chem.* **58**, 390–403 (2020). <https://doi.org/10.1002/mrc.4899>
65. J. Marchand, E. Martineau, Y. Guitton et al., Multidimensional NMR approaches towards highly resolved, sensitive and high-throughput quantitative metabolomics. *Curr. Opin. Biotechnol.* **43**, 49–55 (2017). <https://doi.org/10.1016/j.copbio.2016.08.004>
66. P. Schanda, Fast-pulsing longitudinal relaxation optimized techniques: enriching the toolbox of fast biomolecular NMR spectroscopy. *Prog. Nucl. Magn. Reson. Spectrosc.* **55**, 238–265 (2009). <https://doi.org/10.1016/j.pnmrs.2009.05.002>
67. E.R.F. Kupce, Fast multidimensional NMR by polarization sharing. *Magn. Reson. Chem.* **45**, 2–4 (2007). <https://doi.org/10.1002/mrc.1931>
68. B. Vitorge, G. Bodenhausen, P. Pelupessy, Speeding up nuclear magnetic resonance spectroscopy by the use of SMALL Recovery Times—SMART NMR. *J. Magn. Reson.* **207**, 149–152 (2010). <https://doi.org/10.1016/j.jmr.2010.07.017>
69. M. Quinternet, J.P. Starck, M.A. Delsuc, B. Kieffer, Heteronuclear NMR provides an accurate assessment of therapeutic insulin's quality. *J. Pharm. Biomed. Anal.* **78–79**, 252–254 (2013). <https://doi.org/10.1016/j.jpba.2013.02.016>

70. M. D'Onofrio, L. Ragona, D. Fessas et al., NMR unfolding studies on a liver bile acid binding protein reveal a global two-state unfolding and localized singular behaviors. *Arch. Biochem. Biophys.* **481**, 21–29 (2009). <https://doi.org/10.1016/j.abb.2008.10.017>
71. M. Pathan, S. Akoka, I. Tea, B. Charrier, P. Giraudeau, “Multi-scan single shot” quantitative 2D NMR: a valuable alternative to fast conventional quantitative 2D NMR. *Analyst* **136**, 3157–3163 (2011). <https://doi.org/10.1039/c1an15278e>
72. E. Martineau, P. Giraudeau, I. Tea, S. Akoka, Fast and precise quantitative analysis of metabolic mixtures by 2D 1H INADEQUATE NMR. *J. Pharm. Biomed. Anal.* **54**, 252–257 (2011). <https://doi.org/10.1016/j.jpba.2010.07.046>
73. T. Jézéquel, C. Deborde, M. Maucourt et al., Absolute quantification of metabolites in tomato fruit extracts by fast 2D NMR. *Metabolomics* **11**, 1231–1242 (2015). <https://doi.org/10.1007/s11306-015-0780-0>
74. S. Akoka, P. Giraudeau, Fast hybrid multi-dimensional NMR methods based on ultrafast 2D NMR. *Magn. Reson. Chem.* **53**, 986–994 (2015). <https://doi.org/10.1002/mrc.4237>
75. A.L. Guennec, I. Tea, I. Antheaume et al., Fast determination of absolute metabolite concentrations by spatially encoded 2D NMR: application to breast cancer cell extracts. *Anal. Chem.* **84**, 10831–10837 (2012). <https://doi.org/10.1021/ac3033504>
76. I. Timári, C. Wang, A.L. Hansen et al., Real-time pure shift HSQC NMR for untargeted metabolomics. *Anal. Chem.* **91**, 2304–2311 (2019). <https://doi.org/10.1021/acs.analchem.8b04928>
77. D. Uhrín, T. Liptaj, K.E. Kövér, Modified BIRD pulses and design of heteronuclear pulse sequences. *J. Magn. Reson. Ser. A* **101**, 41–46 (1993)
78. N.M. Byers, A.C. Fleshman, R. Perera, C.R. Molins, Metabolomic insights into human arboviral infections: dengue, chikungunya, and zika viruses. *Viruses* **11**, 1–30 (2019). <https://doi.org/10.3390/v11030225>
79. E.C. da Nunes, G.A.B. Canuto, Metabolomics applied in the study of emerging arboviruses caused by *Aedes aegypti* mosquitoes: a review. *Electrophoresis* **41**, 2102–2113 (2020). <https://doi.org/10.1002/elps.202000133>
80. V. Tounta, Y. Liu, A. Cheyne, G. Larrouy-Maumus, Metabolomics in infectious diseases and drug discovery. *Mol. Omi.* **17**, 376–393 (2021). <https://doi.org/10.1039/d1mo00017a>
81. H. Zheng, M. Chen, S. Lu et al., Metabolic characterization of hepatitis B virus-related liver cirrhosis using NMR-based serum metabolomics. *Metabolomics* **13**, 1–9 (2017). <https://doi.org/10.1007/s11306-017-1260-5>
82. M.M.G. Godoy, E.P.A. Lopes, R.O. Silva et al., Hepatitis C virus infection diagnosis using metabolomics. *J. Viral. Hepat.* **17**, 854–858 (2010). <https://doi.org/10.1111/j.1365-2893.2009.01252.x>
83. S. Wei, Y. Suryani, G.A.N. Gowda et al., Differentiating hepatocellular carcinoma from hepatitis C using metabolite profiling. *Metabolites* **2**, 701–716 (2012). <https://doi.org/10.3390/metabo2040701>
84. N. Embade, O. Millet, Molecular determinants of chronic liver disease as studied by NMR-metabolomics. *Curr. Top. Med. Chem.* **17**, 2752–2766 (2017). <https://doi.org/10.2174/1568026617666170707124539>
85. L.R. Gouveia, J.C. Santos, R.D. Silva et al., Diagnosis of coinfection by schistosomiasis and viral hepatitis B or C using 1H NMR-based metabolomics. *PLoS ONE* **12**, 1–11 (2017). <https://doi.org/10.1371/journal.pone.0182196>
86. G. Meoni, S. Lorini, M. Monti et al., The metabolic fingerprints of HCV and HBV infections studied by nuclear magnetic resonance spectroscopy. *Sci. Rep.* **9**, 1–13 (2019). <https://doi.org/10.1038/s41598-019-40028-4>
87. M. Shannuganathan, M.O. Sarfaraz, Z. Kroezen et al., A cross-platform metabolomics comparison identifies serum metabolite signatures of liver fibrosis progression in chronic hepatitis C patients. *Front. Mol. Biosci.* **8**, 1–15 (2021). <https://doi.org/10.3389/fmolb.2021.676349>
88. C.M. Slupsky, K.N. Rankin, H. Fu et al., Pneumococcal pneumonia: potential for diagnosis through a urinary metabolic profile. *J. Proteome. Res.* **8**, 5550–5558 (2009). <https://doi.org/10.1021/pr9006427>

89. S.U. Munshi, S. Taneja, N.S. Bhavesh et al., Metabonomic analysis of hepatitis e patients shows deregulated metabolic cycles and abnormalities in amino acid metabolism. *J. Viral. Hepat.* **18** (2011). <https://doi.org/10.1111/j.1365-2893.2011.01488.x>
90. R. Hewer, J. Vorster, F.E. Steffens, D. Meyer, Applying biofluid 1H NMR-based metabonomic techniques to distinguish between HIV-1 positive/AIDS patients on antiretroviral treatment and HIV-1 negative individuals. *J. Pharm. Biomed. Anal.* **41**, 1442–1446 (2006). <https://doi.org/10.1016/j.jpba.2006.03.006>
91. S.U. Kaur, B.F. Oyeyemi, A. Shet et al., Plasma metabolomic study in perinatally HIV-infected children using 1H NMR spectroscopy reveals perturbed metabolites that sustain during therapy. *PLoS ONE* **15**, 1–17 (2020). <https://doi.org/10.1371/journal.pone.0238316>
92. T.R. McKnight, H.A.I. Yoshihara, L.J. Sitole et al., A combined chemometric and quantitative NMR analysis of HIV/AIDS serum discloses metabolic alterations associated with disease status. *Mol. Biosyst.* **10**, 2889–2897 (2014). <https://doi.org/10.1039/c4mb00347k>
93. C. Philippeos, F.E. Steffens, D. Meyer, Comparative 1H NMR-based metabonomic analysis of HIV-1 sera. *J. Biomol. NMR* **44**, 127–137 (2009). <https://doi.org/10.1007/s10858-009-9329-8>
94. E. Rodríguez-Gallego, J. Gómez, P. Domingo et al., Circulating metabolomic profile can predict dyslipidemia in HIV patients undergoing antiretroviral therapy. *Atherosclerosis* **273**, 28–36 (2018). <https://doi.org/10.1016/j.atherosclerosis.2018.04.008>
95. L.J. Sitole, F. Tugizimana, D. Meyer, Multi-platform metabolomics unravel amino acids as markers of HIV/combination antiretroviral therapy-induced oxidative stress. *J. Pharm. Biomed. Anal.* **176**, 112796 (2019). <https://doi.org/10.1016/j.jpba.2019.112796>
96. S.U. Munshi, B.B. Rewari, N.S. Bhavesh, S. Jameel, Nuclear magnetic resonance based profiling of biofluids reveals metabolic dysregulation in HIV-infected persons and those on anti-retroviral therapy. *PLoS One* **8** (2013). <https://doi.org/10.1371/journal.pone.0064298>
97. C.D. French, R.E. Willoughby, A. Pan et al., NMR metabolomics of cerebrospinal fluid differentiates inflammatory diseases of the central nervous system. *PLoS Negl. Trop. Dis.* **12**, 1–17 (2018). <https://doi.org/10.1371/journal.pntd.0007045>
98. M.M. Banoei, H.J. Vogel, A.M. Weljie et al., Plasma metabolomics for the diagnosis and prognosis of H1N1 influenza pneumonia. *Crit. Care* **21**, 1–15 (2017). <https://doi.org/10.1186/s13054-017-1672-7>
99. J.L. Izquierdo-Garcia, N. Nin, J. Jimenez-Clemente et al., Metabolomic profile of ards by nuclear magnetic resonance spectroscopy in patients with h1n1 influenza virus pneumonia. *Shock* **50**, 504–510 (2018). <https://doi.org/10.1097/SHK.0000000000001099>
100. N. Shahfiza, H. Osman, T.T. Hock et al., Metabolomics for characterization of gender differences in patients infected with dengue virus. *Asian Pac. J. Trop. Med.* **8**, 451–456 (2015). <https://doi.org/10.1016/j.apjtm.2015.05.012>
101. S.P. Young, M. Nessim, F. Falciani et al., Metabolomic analysis of human vitreous humor differentiates ocular inflammatory disease. *Mol. Vis.* **15**, 1210–1217 (2009)
102. J. Shrinet, J.S. Shastri, R. Gaiind et al., Serum metabolomics analysis of patients with chikungunya and dengue mono/co-infections reveals distinct metabolite signatures in the three disease conditions. *Sci. Rep.* **6**, 1–12 (2016). <https://doi.org/10.1038/srep36833>
103. D.J. Adamko, E. Saude, M. Bear et al., Urine metabolomic profiling of children with respiratory tract infections in the emergency department: a pilot study. *BMC Infect. Dis.* **16** (2016). <https://doi.org/10.1186/s12879-016-1709-6>
104. C. Bruzzzone, S. Lu, T. Diercks et al., in *iScience II SARS-CoV-2 Infection Dysregulates the Metabolomic and Lipidomic Profiles of Serum the Metabolomic and Lipidomic Profiles of Serum* (2020). <https://doi.org/10.1016/j.isci.2020.101645>
105. D.D. Fraser, M. Slessarev, C.M. Martin et al., Metabolomics profiling of critically ill coronavirus disease 2019 patients: identification of diagnostic and prognostic biomarkers. *Crit. Care Explor.* **2**, e0272 (2020). <https://doi.org/10.1097/ccx.0000000000000272>
106. A. Valdés, L.O. Moreno, S.R. Rello et al., Metabolomics study of COVID-19 patients in four different clinical stages. *Sci. Rep.* **12**, 1–11 (2022). <https://doi.org/10.1038/s41598-022-05667-0>

107. E. Holmes, J. Wist, R. Masuda et al., in *Incomplete Systemic Recovery and Metabolic Phenoreversion in Post-Acute-Phase Nonhospitalized COVID-19 Patients: Implications for Assessment of Post-Acute COVID-19 Syndrome* (2021). <https://doi.org/10.1021/acs.jproteome.1c00224>
108. T. Kimhofer, S. Lodge, L. Whiley et al., in *Integrative Modeling of Quantitative Plasma Lipoprotein, Metabolic, and Amino Acid Data Reveals a Multiorgan Pathological Signature of SARS-CoV-2 Infection* (2020). <https://doi.org/10.1021/acs.jproteome.0c00519>
109. F. Schmelter, B. Föh, A. Mallagaray et al., Metabolic and lipidomic markers differentiate COVID-19 from non-hospitalized and other intensive care patients. *Front. Mol. Biosci.* **8**, 1–12 (2021). <https://doi.org/10.3389/fmolb.2021.737039>
110. A.F. Rendeiro, C.K. Vorkas, J. Krumsiek et al., Metabolic and immune markers for precise monitoring of COVID-19 severity and treatment. *Front. Immunol.* **12**, 1–13 (2022). <https://doi.org/10.3389/fimmu.2021.809937>
111. J.A. Lorente, N. Nin, P. Villa et al., Metabolomic differences between COVID-19 and H1N1 influenza induced ARDS. *Crit. Care* **25**, 1–11 (2021). <https://doi.org/10.1186/s13054-021-03810-3>
112. N. Embade, Z. Mariño, T. Diercks et al., Metabolic characterization of advanced liver fibrosis in HCV patients as studied by serum ¹H-NMR spectroscopy. *PLoS ONE* **11**, 1–19 (2016). <https://doi.org/10.1371/journal.pone.0155094>
113. E. Baranovicova, A. Bobcakova, R. Vysehradsky et al., The ability to normalise energy metabolism in advanced covid-19 disease seems to be one of the key factors determining the disease progression—a metabolomic nmr study on blood plasma. *Appl. Sci.* **11**, 4–6 (2021). <https://doi.org/10.3390/app11094231>
114. M. Manchester, A. Anand, in *Metabolomics: Strategies to Define the Role of Metabolism in Virus Infection and Pathogenesis*, 1st edn. (Elsevier Inc., 2017)
115. D.S. Wishart, C. Knox, A.C. Guo et al., HMDB: a knowledgebase for the human metabolome. *Nucleic Acids Res.* **37**, 603–610 (2009). <https://doi.org/10.1093/nar/gkn810>
116. O. Beckonert, H.C. Keun, T.M.D. Ebbels et al., Metabolic profiling, metabolomic and metabolomic procedures for NMR spectroscopy of urine, plasma, serum and tissue extracts. *Nat. Protoc.* **2**, 2692–2703 (2007). <https://doi.org/10.1038/nprot.2007.376>
117. G.F. Giskeødegård, T. Andreassen, H. Bertilsson et al., The effect of sampling procedures and day-to-day variations in metabolomics studies of biofluids. *Anal. Chim. Acta.* **1081**, 93–102 (2019). <https://doi.org/10.1016/j.aca.2019.07.026>
118. A.C. Dona, B. Jiménez, H. Schafer et al., Precision high-throughput proton NMR spectroscopy of human urine, serum, and plasma for large-scale metabolic phenotyping. *Anal. Chem.* **86**, 9887–9894 (2014). <https://doi.org/10.1021/ac5025039>
119. B. Khakimov, N. Mobaraki, A. Trimigno et al., Signature mapping (SigMa): an efficient approach for processing complex human urine ¹H NMR metabolomics data. *Anal. Chim. Acta.* **1108**, 142–151 (2020). <https://doi.org/10.1016/j.aca.2020.02.025>
120. R.W. Evans, Diagnostic testing for headache. *Med. Clin. North. Am.* **85**, 865–885 (2001). [https://doi.org/10.1016/S0025-7125\(05\)70348-5](https://doi.org/10.1016/S0025-7125(05)70348-5)
121. B. Shen, X. Yi, Y. Sun et al., Proteomic and metabolomic characterization of COVID-19 patient sera. *Cell* **182**, 59–72.e15 (2020). <https://doi.org/10.1016/j.cell.2020.05.032>
122. M.R. Hasan, M. Suleiman, A. Pérez-López, Metabolomics in the diagnosis and prognosis of COVID-19. *Front. Genet.* **12** (2021). <https://doi.org/10.3389/fgene.2021.721556>
123. M. Costanzo, M. Caterino, R. Fedele et al., COVIDomics: the proteomic and metabolomic signatures of COVID-19. *Int. J. Mol. Sci.* **23**, 2414 (2022). <https://doi.org/10.3390/ijms23052414>
124. B.S.B. Correia et al., ¹H qNMR based metabolomics discrimination of COVID-19 severity. *J. Proteome. Res.* (in press)
125. V. Khullar, R.J. Firpi, Hepatitis C cirrhosis: new perspectives for diagnosis and treatment. *World J. Hepatol.* **7**, 1843–1855 (2015). <https://doi.org/10.4254/wjh.v7.i14.1843>
126. R.H. Westbrook, G. Dusheiko, Natural history of hepatitis C. *J. Hepatol.* **61**, S58–S68 (2014). <https://doi.org/10.1016/j.jhep.2014.07.012>

127. R.F. Schwabe, J.J. Maher, Lipids in liver disease: Looking beyond steatosis. *Gastroenterology* **142**, 8–11 (2012). <https://doi.org/10.1053/j.gastro.2011.11.004>
128. F.S. Macaluso, M. Maida, M.G. Minissale et al., Metabolic factors and chronic hepatitis C: a complex interplay. *Biomed. Res. Int.* 2013 (2013). <https://doi.org/10.1155/2013/564645>